

## **A Proposed Radar Strategy for the Prediction and Warning of Severe Hail Using Polarimetric Radar Data**

*Ian Lee\**

*NOAA/National Weather Service  
Albany, New York*

### **ABSTRACT**

*Ground-truth observations play a crucial role in the issuance of National Weather Service (NWS) Severe Thunderstorm Warnings for severe hail. Many radar warning techniques for severe hail are created off of these ground-based observations, which are correlated to quantitative threshold values that were observed at the time of severe hail occurrence. With the inclusion of Polarimetric radar (PR) data into NWS warning operations, the sampling of hydrometeors in both the horizontal and vertical provides the opportunity to discern amongst different hydrometeor types in the mixed phase region of a thunderstorm updraft. Used in conjunction with an understanding of thunderstorm dynamics and the surrounding thermodynamic and kinematic environment, PR data can provide the ability to forecast the occurrence of severe hail at the ground early in the lifecycle of a thunderstorm. A proposed strategy and decision aid are introduced that outline a qualitative conceptual forecast approach to the issuance of Severe Thunderstorm Warnings for severe hail using PR data. Applications of this approach are provided for two thunderstorms that occurred during the 21 May 2013 severe weather event across the NWS Albany, New York county warning area.*

---

---

\*Corresponding author address: Ian Lee, NOAA/NWS 251 Fuller Rd. Suite B300 Albany, New York 12203. E-Mail: [ian.lee@noaa.gov](mailto:ian.lee@noaa.gov)

## 1. Introduction

Over the past couple of decades, technological advancements in radar meteorology have led to improved detection of severe hail when issuing National Weather Service (NWS) Severe Thunderstorm Warnings. The installation of Polarimetric radar (PR) capabilities at NWS WSR-88D radars beginning in the spring of 2011 led to further advancements by allowing hydrometeors to be sampled in both the horizontal and vertical dimensions, whereas legacy (pre-PR) radar data only sampled hydrometeors in the horizontal dimension ([Radar Operations Center 2013](#)). With the capability of horizontal and vertical sampling, hydrometeor shape and orientation can be resolved to provide a determination of detected particle type ([Rinehart 2010](#)).

Prior to PR data, legacy radar data were used to develop warning techniques to issue Severe Thunderstorm Warnings for severe hail. These legacy radar techniques are observation-based, with the occurrence of severe hail, 2.5 cm (1.0 in) in diameter ([NWS Directive 10-511](#)), correlated to observed radar values used as thresholds during the warning process. Recent studies, such as [Kramar and Waters \(2009\)](#), have begun to take into account thermodynamic effects by examining factors such as the freezing level. Local NWS office county warning area (CWA) meteorological and topographical characteristics have also been considered through local and regional studies ([Cerniglia and Snyder 2002](#); [Lahiff 2005](#); [Porter et al. 2005](#); [Donavon and Jungbluth 2007](#); [Hayes 2008](#); [Frugis and Wasula 2011](#) and others).

With the advent of PR data, new diagnostic techniques incorporating the PR base variables of differential reflectivity ( $Z_{DR}$ ), correlation coefficient ( $\rho_{hv}$ , hereafter CC), and specific differential phase ( $K_{DP}$ ) have been developed to help improve hail detection and size estimation ([Kumjian 2013a](#)). Recent technological advancements such as the Four-Dimensional Storm Investigator (FSI) have also provided for quick and efficient methods to analyze multiple thunderstorms capable of producing severe hail ([Stumpf et al. 2006](#)).

The use of PR data in the warning process can allow for a different approach to issuing Severe Thunderstorm Warnings for severe hail. With PR data sampling hydrometeors in both the horizontal and vertical, the warning process can be approached through a conceptual framework that favors a forecast methodology over numerical thresholds in the warning process. By tracking various PR features through time with a conceptual understanding of the numerical output, the prediction of severe hail at the ground early in a thunderstorm lifecycle can be achieved given favorable thunderstorm dynamics and thermodynamic and kinematic environments. A proposed radar warning strategy and decision aid are introduced providing a conceptual forecast approach to the issuance of Severe Thunderstorm Warnings for severe hail using PR data. Applications of this approach are provided for two thunderstorms that occurred during the 21 May 2013 severe weather event across the NWS Albany, New York (NY) county warning area ([Fig. 1](#)).

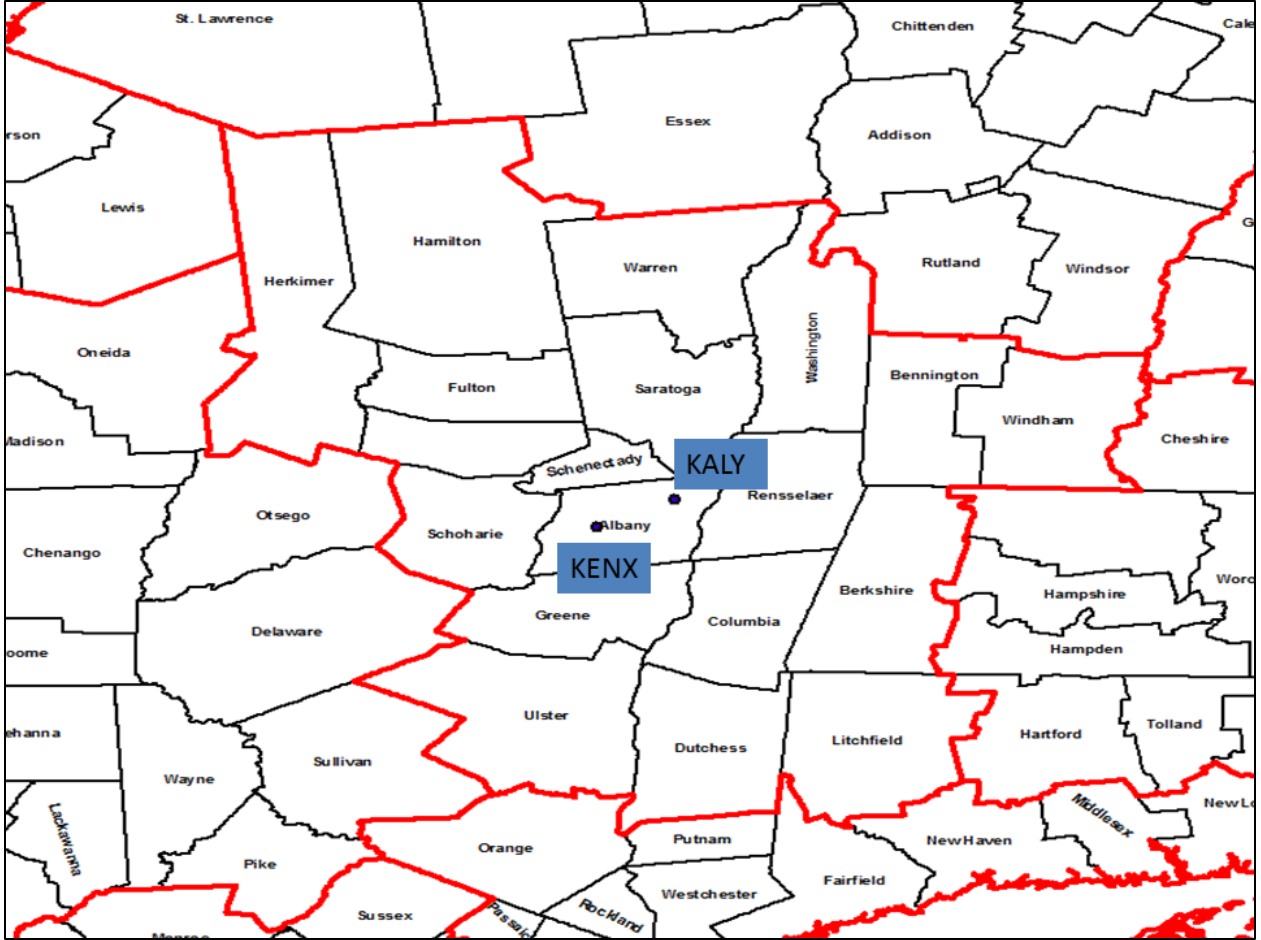


**Fig. 1.** NWS Albany, NY upper air (KALY) and WSR-88D (KENX) locations within the KALY CWA. Orange lines denote CWA boundaries and black lines denote county boundaries.

## 2. Background

Current legacy radar warning techniques for severe hail require an analysis of numerical radar output compared to a known set of thresholds, with these threshold values determined from past observed severe hail events. As part of these techniques, it can be inferred that there is a direct relationship between hail size and apparent thunderstorm updraft strength as measured through the anelastic continuity equation, which relates vertical velocity to horizontal divergence ([Witt and Nelson 1991](#), hereafter WN91):

$$\nabla \cdot Vh + \frac{\partial \omega}{\partial z} + \omega \frac{\partial \ln p}{\partial z} = 0 \quad (1)$$

Integrating this equation in the vertical implies that stronger updraft velocities occur in environments of supportive horizontal divergence in the anvil layer, which can be inferred by increasing values of storm-top divergence that occur in environments of favorable low-level convergence and upper-level divergence ([WN91](#); [Bousted 2008](#)). Further enhancing updraft velocity can be the amount of Convective Available Potential Energy (CAPE) available in the thermodynamic environment to add buoyancy to a parcel traveling through an

updraft, with stronger updraft velocities correlated to increased values of CAPE ([Holton 1992](#)):

$$W_{\max} = \sqrt{2CAPE} \quad (2)$$

An additional thermodynamic factor that can increase parcel buoyancy in a thunderstorm updraft is a steep mid-level lapse rate, with hail more likely in environments favorable for evaporative cooling (dry air entrainment), and sufficient low-level moisture ([Johns and Doswell 1992](#), hereafter JD92).

Similarly, the probability for hail can be related to thunderstorm depth, with taller and deeper updrafts more likely to reside in temperatures cold enough to promote hail formation in the hail growth zone of -10°C to -30°C, especially during the warm season ([Miller et al. 1988](#)). In environments favorable for melting of hail below the beam, PR data can be analyzed relative to the -10°C to -30°C layer, as this hail growth zone applies to all thunderstorms ([Miller et al. 1988](#)). However, this zone can be expanded to temperatures as warm as -8°C to account for different ice nuclei that may be present in a thunderstorm updraft ([Markowski and Richardson 2010](#), hereafter MR10). Kinematics can also play a large role, with sufficient environmental shear promoting recycling processes due to nonhydrostatic pressure effects that can enhance storm-scale rotation and mesocyclone strength ([Miller et al. 1988](#); [JD92](#)).

Using the numerical output of PR data conceptually, various PR features can be correlated to specific temperature levels favorable in the hail formation process.  $Z_{DR}$  columns, in which  $Z_{DR}$  values of at least 1.0 dB extend above the 0°C level, can be an indicator of robust updrafts capable of

lofting liquid water droplets that could then become supercooled and used in the hail formation process ([Kumjian and Ryzhkov 2008](#), hereafter KR08).  $K_{DP}$  columns, a direct measure of the liquid water content (LWC) available in an updraft, of at least 1.0 deg/km above the -10°C level ([KR08](#)) can be an indicator of sufficient LWC necessary to promote hail growth within the hail growth zone of -10°C to -30°C ([Miller et al. 1988](#)). Similarly, taller  $Z_{DR}$  and  $K_{DP}$  columns that reach well into the hail growth zone can be further indicative of strong updrafts that are capable of lofting liquid water and supercooled water droplets for the formation of hail. Low CC updraft cores can be indicative of updrafts in which mixed phase hydrometeors are present aloft within the hail growth zone ([KR08](#)), with anomalously low values potentially indicating large hailstones ([Picca and Ryzhkov 2012](#)).

The presence of other PR signatures can also be used in the warning process. Rotating thunderstorms with particularly strong updrafts may exhibit mesocyclones with a  $Z_{DR}$  and/or CC ring of higher values around the updraft core ([Kumjian 2013b](#)). Water-coated hail, evident by high values of  $K_{DP}$  (2.0+ deg/km), can reflect a thermodynamic environment supportive of melting hail processes ([Kumjian 2013b](#)). Three-Body Scatter Spikes (TBSS), shown by anomalous values of  $Z_{DR}$  and CC, may also be present down radial of a high reflectivity echo contaminated by Mie scattering of large hailstones ([Lemon 1998](#)) and enhanced by anomalous values of  $Z_{DR}$  and CC ([Straka et al. 2000](#)). Other radar features such as weak echo regions and bounded weak echo regions can also be used as a rough proxy for updraft strength as well ([Lemon 1977](#)).

### 3. Methodology

Using PR data in the warning process, in conjunction with a conceptual understanding of thunderstorm updraft dynamics and a situational awareness of the thermodynamic and kinematic environment, a qualitative approach can be developed to forecast the potential for severe hail at the ground early in the lifecycle of a thunderstorm. [Figure 2](#) depicts a decision aid that outlines this process, split into three thunderstorm updraft stages that outline the updraft growth and hail formation process.

To analyze PR data using the decision aid, FSI can be utilized. It is recommended that the Constant Altitude Plan Position Indicator (CAPPI) be initially set at the 0°C level, obtained from either a proximity sounding or the latest available model sounding of choice. The CAPPI can also be adjusted to the -10°C and -20°C levels throughout the decision aid to assess thunderstorm updraft strength. Similarly, the Vertical Dynamic XSection (VDX) can be used with the “Sampling” feature turned on to assess the vertical structure of an updraft. The Plan Position Indicator (PPI) can be used to examine the lowest elevation angle, typically 0.5° ([Stumpf et al. 2004](#)).

To maintain adequate situational awareness while using the decision aid, it is recommended to assess the thermodynamic and kinematic environment beforehand. A suggested favorable thermodynamic environment for hail includes: sufficient instability as measured through variables such as CAPE and mid-level lapse rates, mid-level evaporative cooling due to dry air entrainment, and sufficient low-level moisture ([Holton 1992](#); [JD92](#)). A suggested favorable kinematic environment includes sufficient shear to support updraft sustainment to deter precipitation loading, although storm-scale rotation is not required

([Miller et al. 1988](#); [JD92](#)). The above suggestions are not all-encompassing, with local CWA characteristics and environmental factors that can also be taken into consideration.

#### *a) Stage 1 – Updraft Development and Hail Formation*

To assess the potential for hail formation in a developing thunderstorm updraft, the height of the  $Z_{DR}$  column, and to a lesser extent  $K_{DP}$  column, must reach or exceed the 0°C level in order for liquid water droplets to be available for the hail formation process ([KR08](#)). During this stage, although not necessary on the lowest elevation slice, 50-60 dBZ echoes may become apparent signifying the growth of liquid water droplets into larger rain droplets ([Straka et al. 2000](#)). CC values may become slightly depressed (0.95-0.99) above the 0°C level, indicative of a mixture of small and large rain droplets interspersed with developing hail embryos ([Straka et al. 2000](#)). Thunderstorm updrafts that do not have  $Z_{DR}$  and  $K_{DP}$  columns reaching the 0°C level will not have liquid water droplets available at subfreezing temperatures, and instead will resemble warm rain processes.

It is recommended that the FSI CAPPI be set to the 0°C level during Stage 1 to assess thunderstorm updraft strength and the ability to loft liquid water droplets into subfreezing temperatures. Depending on the favorability of the thermodynamic and kinematic environments and if the  $Z_{DR}/K_{DP}$  columns extend or exceed the 0°C level, a Special Weather Statement may be issued at this time with the expectation of subsevere hail forming from the development of small hailstones that have had sufficient residence time within the updraft before reaching the ground ([NWS Directive 10-517](#)).



*b) Stage 2 – Updraft Growth and Hail Growth*

As updraft growth continues, the  $Z_{DR}$  and  $K_{DP}$  columns will continue to grow in vertical depth above the  $0^{\circ}\text{C}$  level signifying that supercooled water droplets are being lofted further into the updraft (KR08). For supercooled water droplets to be available for the growth of hailstones, the  $Z_{DR}$  and  $K_{DP}$  columns must extend to the  $-10^{\circ}\text{C}$  level in order for supercooled water droplets to be available within the hail growth zone of  $-10^{\circ}\text{C}$  to  $-30^{\circ}\text{C}$  (Miller et al. 1988; Straka et al. 2000). The  $-10^{\circ}\text{C}$  level is not a static level, however, as heterogeneous ice nucleation processes can allow for hail growth at temperatures as warm as  $-8^{\circ}\text{C}$  (MR10). It is recommended that the FSI CAPPI be set at the  $-10^{\circ}\text{C}$  level during Stage 2, as this level is often considered the beginning of the mixed phase region within a thunderstorm updraft, although the  $Z_{DR}$  and  $K_{DP}$  columns may be as high as the  $-20^{\circ}\text{C}$  level depending on the strength of the updraft (Miller et al. 1988; Straka et al. 2000).

As supercooled water droplets are lofted into the mixed phase region of a thunderstorm updraft, CC values can be used as an indication hailstones are beginning to increase in size (Scharfenberg et al. 2005). In the early stages of hail formation, CC will begin to lower into the 0.90-0.95 range first around the  $-10^{\circ}\text{C}$  level (KR08). This region of depressed CC values may extend past the  $-10^{\circ}\text{C}$  level depending on the strength of the updraft. A possible reason for the initial depression in CC values is the generation of small hailstones that have not had enough residence time within the updraft (Hubbert et al. 1998).

Early signs of storm-scale rotation can provide greater confidence that

hailstones will continue to grow in size as recycling processes due to nonhydrostatic pressure differences contribute to the hail growth process (Thompson et al. 2003). Although storm-scale rotation can help promote hail formation and growth, it is not required as pulse thunderstorms typically exhibit little if any storm-scale rotation (Lemon 1977). During this stage, 50-65 dBZ echoes will also increase in vertical depth and become apparent on the lowest elevation slice as rain mixed with small, subsevere hail falls at the ground.  $Z_{DR}$  values will remain generally greater than 1.0 dB, along with slightly depressed CC values between 0.90-0.99 (Straka et al. 2000).  $K_{DP}$  values will depend on the amount of moisture available in the thermodynamic environment and will generally be 0.5 deg/km or greater (Straka et al. 2000).

Monitoring storm trends and depending on the favorability of the thermodynamic and kinematic environments, a Severe Thunderstorm Warning should be issued at this time (NWS Directive 10-511). The warning can be issued at this time based on the forecast that severe hail will occur at the ground given the conceptual forecast approach taken in analyzing a thunderstorm updraft using PR data. With the  $Z_{DR}$  and  $K_{DP}$  columns at or above the  $-10^{\circ}\text{C}$  level, a thunderstorm updraft in a favorable environment will continue to supply supercooled water droplets into the hail growth zone allowing for an extended duration of hail growth to severe limits. Thunderstorm updrafts that have  $Z_{DR}$  and  $K_{DP}$  columns remaining below the  $-10^{\circ}\text{C}$  level, but above the  $0^{\circ}\text{C}$  level, can still support the formation of hail embryos and small hailstones, but will likely be subsevere without extending into the hail growth zone.

Studies such as Changnon (1970) have shown that a full-grown hailstone can take as much as 10 minutes to fall out of a

thunderstorm updraft and reach the surface. A lead time greater than 10 minutes may be possible as well as the Severe Thunderstorm Warning is issued before the hailstones are fully grown. Other factors such as hailstone size and fall speed can additionally affect the time it takes for hailstones to reach the surface ([Matson and Huggins 1980](#), hereafter MH80). The eventual time it takes for hailstones to fall out of a thunderstorm updraft and reach the surface also depends on the updraft strength and near-storm environment ([Miller et al. 1988](#)).

*c) Stage 3 – Updraft Sustainment and Hail Occurrence*

As a thunderstorm updraft continues to grow and/or reaches its peak intensity, 60-65+ dBZ echoes will become apparent in the mixed phase region of the updraft and also possibly at the surface. Studies indicate that thunderstorms with reflectivities of at least 60 dBZ in the lowest elevation slice suggest the presence of hail ([Witt 1996](#)), and 60 dBZ reflectivity echoes  $\geq -20^{\circ}\text{C}$  level signifying the presence of severe hail ([Lemon 1998](#)). The deviation of the 60 dBZ echo top from the  $-20^{\circ}\text{C}$  level can also be indicative of updraft strength, with larger deviations above the  $-20^{\circ}\text{C}$  level correlating to stronger updrafts ([Lemon 1977](#)).  $Z_{\text{DR}}$  and  $K_{\text{DP}}$  columns will also continue to grow and be at their greatest vertical depth with columns as high as the  $-20^{\circ}\text{C}$  level possible, with taller columns correlated to increased updraft strength ([KR08](#)). During this stage, the FSI CAPPI can be set anywhere between the  $-10^{\circ}\text{C}$  and  $-20^{\circ}\text{C}$  levels to assess thunderstorm updraft strength.

Depending on the type of thunderstorm, storm-scale rotation may also be enhanced signifying the presence of a mesocyclone capable of suspending and recycling hailstones within the updraft ([Lemon 1977](#); [Miller et al. 1988](#)). Hail

growth will be most evident by examining the CC values within the updraft core and hail growth zone of  $-10^{\circ}\text{C}$  to  $-30^{\circ}\text{C}$ , with the region of depressed CC values extending from the  $-10^{\circ}\text{C}$  level to as high as the  $-20^{\circ}\text{C}$  level depending on the strength of the updraft ([Miller et al. 1988](#); [KR08](#)). CC values will continue to depress further and be at their lowest values ( $\leq 0.90$ ) reflecting the growth of hailstones to severe limits, ([Straka et al. 2000](#); [KR08](#)) with anomalously low values potentially indicating large hailstones ([Picca and Ryzhkov 2012](#)). Low CC values may also be present in other regions of the thunderstorm as well with hailstones removed from the updraft core given the degree of environmental shear and storm-scale rotation present.

$K_{\text{DP}}$  values will ultimately be dependent on the CC values, with  $K_{\text{DP}}$  unavailable where CC values are  $< 0.90$  ([WDTB 2013](#)). In regions where  $K_{\text{DP}}$  may still be visible, high  $K_{\text{DP}}$  values ( $\geq 2.0$  deg/km) can be indicative of melting hail and/or water coated hail ([Straka et al. 2000](#); [KR08](#)). Other PR features may also become apparent, such as a TBSS or  $Z_{\text{DR}}/\text{CC}$  ring, and can further increase the likelihood that severe hailstones are located in the updraft ([Lemon 1998](#); [Kumjian 2013b](#)).

When the severe hailstones reach a large enough size that they begin to dominate the hydrometeor distribution during Stage 3,  $Z_{\text{DR}}$  values will drop off coincident with a region of depressed CC values on the lowest elevation slice. Base reflectivity values will also be at their highest (60-65+ dBZ).  $Z_{\text{DR}}$  values will drop below 1.0 dB, with the value depending on the size and orientation of the hailstones.  $Z_{\text{DR}}$  values dropping to near 0 dB can also be an indication of the presence of larger hailstones. At the same time, CC will bottom out ( $< 0.90$ ) and  $K_{\text{DP}}$  values (that are not unavailable in regions where  $\text{CC} \leq 0.90$ )

may also remain high, especially if the hailstones are coated with water (Straka et al. 2000).

The strength of the updraft and favorability of the thermodynamic and kinematic environments will ultimately determine the hailstone residence time and maximum potential size, along with the eventual time it takes for severe hailstones to reach the surface (Miller et al. 1988). Near the end of the thunderstorm lifecycle, once the hailstones reach a critical mass, the

updraft will be unable to support the weight of the hailstones and other hydrometeors, causing the updraft to collapse via precipitation loading (Miller et al. 1988). The height of various echo tops,  $Z_{DR}$  and  $K_{DP}$  columns, and depressed CC region will begin to collapse towards the surface as the thunderstorm becomes downdraft-dominated. However, a new thunderstorm updraft may develop nearby, especially in environments favoring multicells and/or supercells.

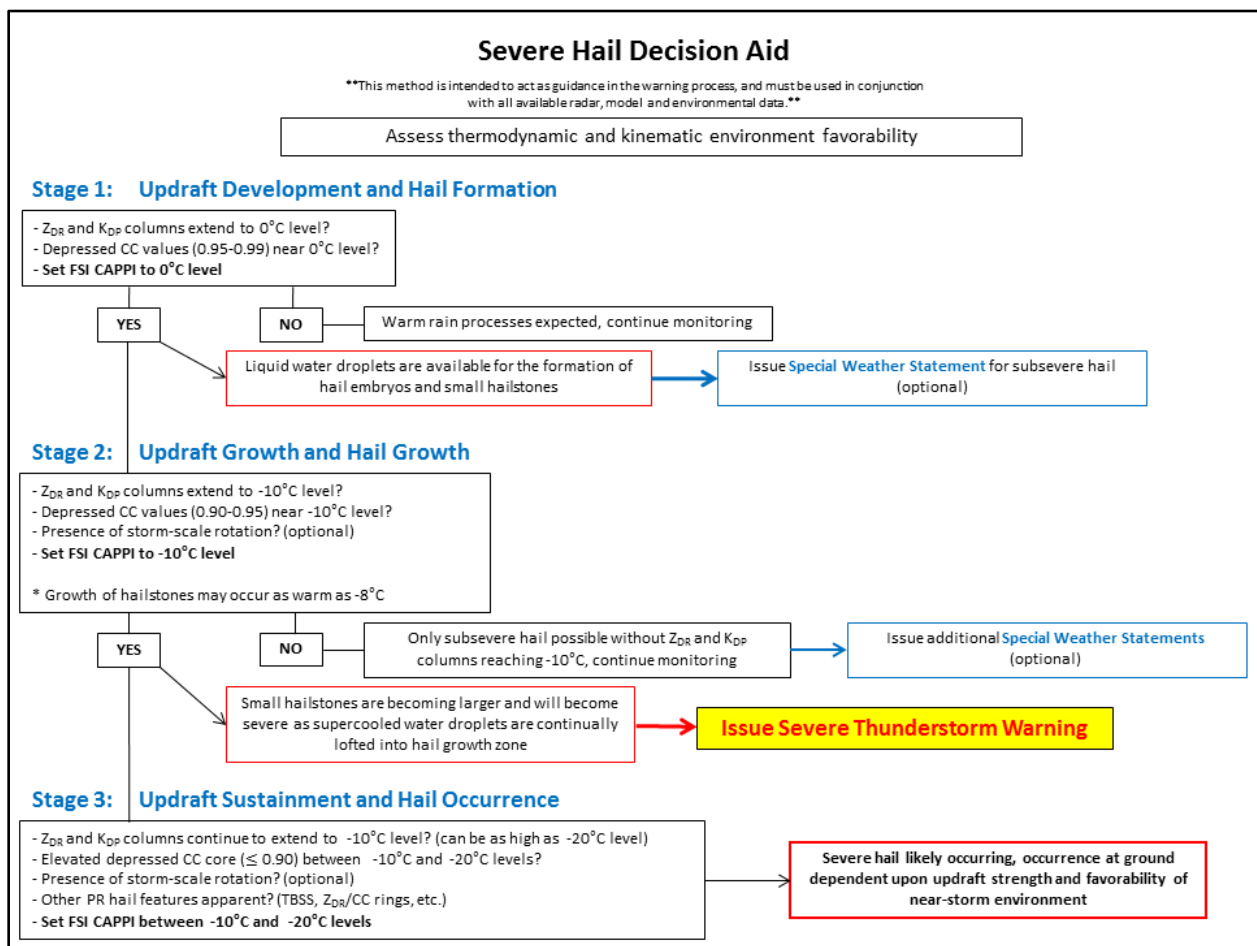


Fig. 2. Severe hail radar decision aid.



#### 4. Applications

The two thunderstorms analyzed from the 21 May 2013 severe weather event formed in a thermodynamic and kinematic environment conducive for severe hail. [Figure 3](#) depicts the synoptic pattern, characterized by a northwest flow regime that featured a 500 hPa ridge axis located across the eastern Great Lakes ([Fig. 3a](#)). This setup allowed for southwesterly return flow at 850 hPa to transport a warm and humid airmass across the Northeast U.S. with 850 hPa temperatures near 16°C and dewpoints in the 12-15°C range ([Fig. 3b](#)). A belt of stronger jet stream westerlies at 300 hPa was located to the north allowing for much of the Northeast U.S. to be under the favorable right entrance region of this upper-level jet streak ([Fig. 3c](#)). A weak frontal boundary and wave of low pressure oriented east-west across the NWS Albany NY CWA was located at the surface providing a trigger for convection ([Fig. 3d](#)).

[Figure 4](#) depicts the 1200 UTC KALY sounding, modified using 1800 UTC surface temperature and dewpoint observations utilizing the NSHARP workstation ([Hart and Korotky 1991](#)). The sounding revealed deep low-level moisture, with a precipitable water (PW) value of 3.78 cm (1.49 in) corresponding to the 75<sup>th</sup> percentile anomaly based off the KALY upper air PW climatology ([NWS Precipitable Water Plots](#)). Strong instability was present, with a Most Unstable Convective Available Potential Energy (MUCAPE) value of 3418 J/kg amidst fairly steep mid-level lapse rates in the 700-500 hPa layer of 6.7°C/km. Dry air was also located in the hail growth zone supporting evaporative cooling processes. Sufficient environmental shear was also present, with 32 knots of bulk shear in the 0-6 km layer. The 0°C level, -10°C level, and -20°C level were located at 3.78 km (12.4 kft), 5.67 km (18.6 kft), and 7.10 km (23.3 kft) respectively.

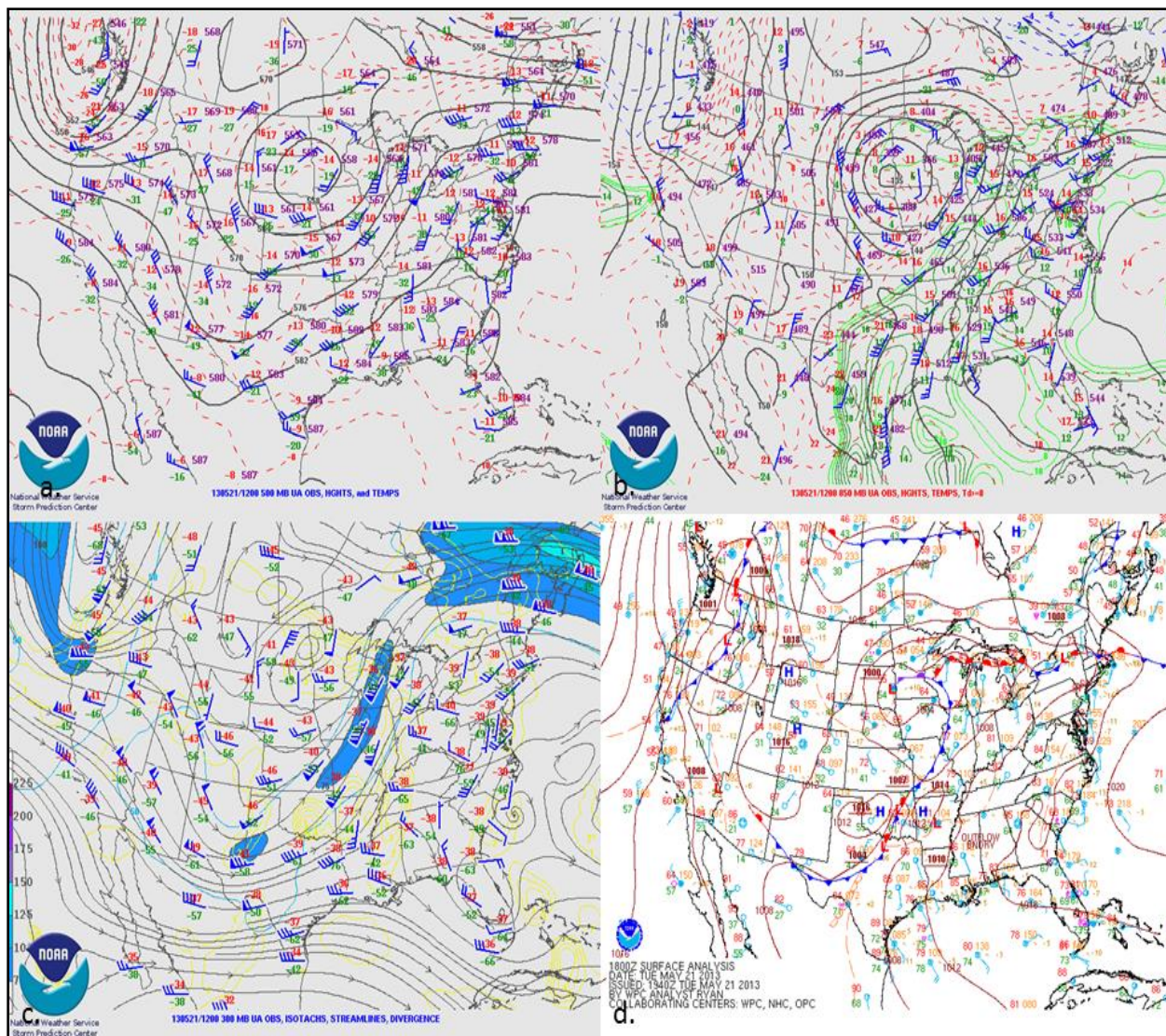


**Fig. 3.** (a) 1200 UTC 21 May 2013 [Storm Prediction Center](#) 500 hPa analysis, (b) 850 hPa analysis, (c) 300 hPa analysis, and (d) [Weather Prediction Center](#) surface pressure and fronts analysis from 1800 UTC 21 May 2013.



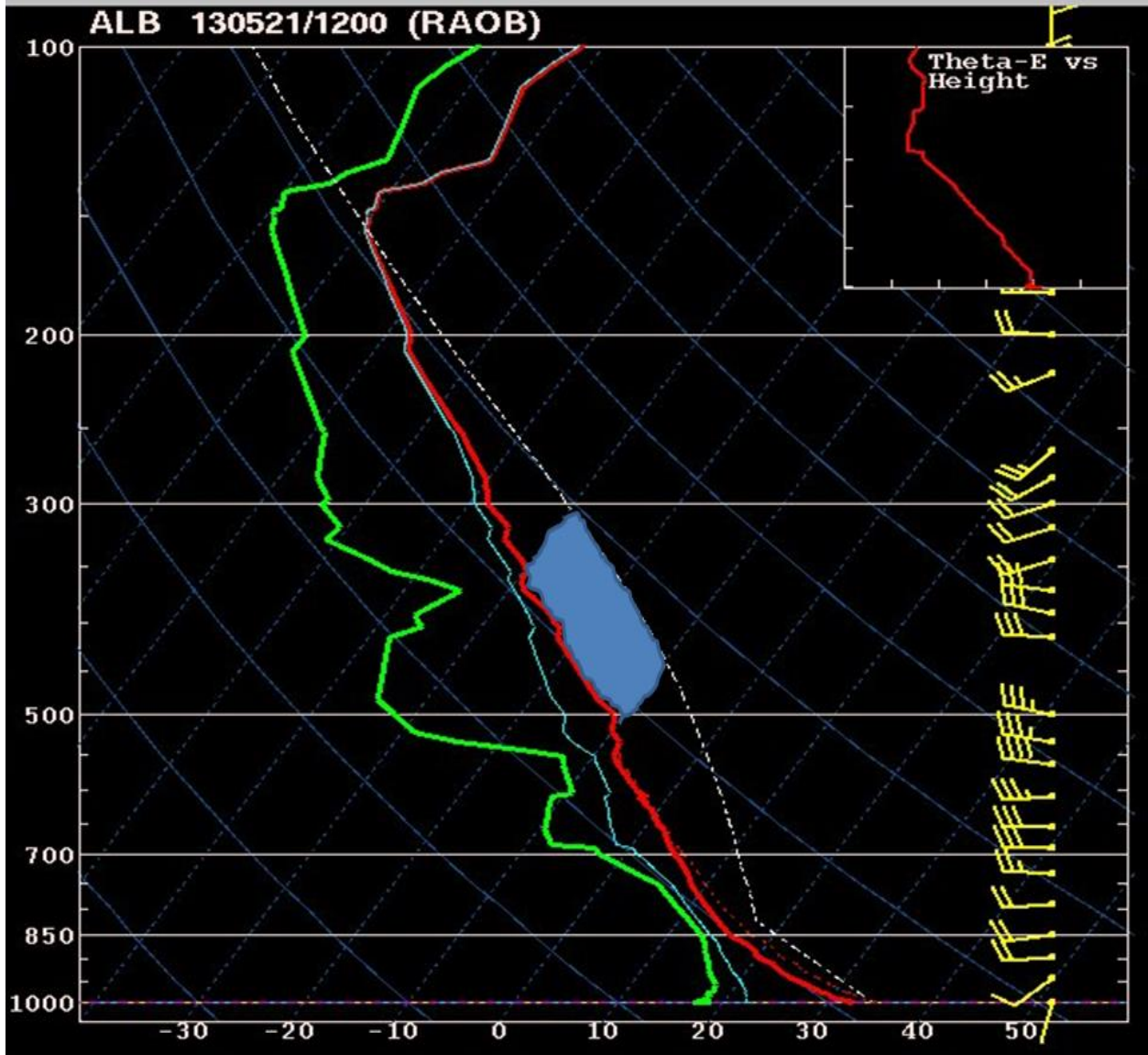


**Fig. 4.** 21 May 2013 KALY 1800 UTC sounding modified using NSHARP ([Hart and Korotky 1991](#)). Shaded region represents available CAPE within the hail growth zone of  $-10^{\circ}\text{C}$  to  $-30^{\circ}\text{C}$  ([Miller et al. 1988](#)).

*a) Case 1: Columbia County, NY*

The first thunderstorm analyzed affected portions of Columbia County in east-central NY between 2024-2047 UTC. [Figures 5-7](#) depict the thunderstorm at Stage 1 of the decision aid ([Fig. 2](#)) at 2024 UTC, with white circles denoting areas of interest. At 2024 UTC, the thunderstorm was in the

updraft development and hail formation stage, with 50 dBZ echoes evident on the lowest elevation slice ([Fig. 5a](#)) and aloft in the updraft core extending from the  $0^{\circ}\text{C}$  level to the  $-20^{\circ}\text{C}$  level ([Fig. 7a](#)). Both the  $Z_{\text{DR}}$  ([Fig. 7b](#)) and  $K_{\text{DP}}$  columns ([Fig. 7d](#)) extend to the  $-10^{\circ}\text{C}$  level, well past the  $0^{\circ}\text{C}$  level. A depressed region of CC values (0.95-0.99) extends from the  $0^{\circ}\text{C}$  level to the

-10°C level indicative of mixed phase hydrometeors present in the updraft core ([Fig. 7c](#)).

Using the decision aid with the FSI CAPPI set at the 0°C level, this thunderstorm is capable of lofting liquid water droplets into subfreezing temperatures for the formation of hail embryos and small hailstones. The  $Z_{DR}$  ([Fig. 6b](#)) and  $K_{DP}$  columns ([Fig. 6d](#)) easily reach the 0°C level, with liquid water droplets readily available for the formation of hail embryos and small hailstones. With depressed CC values in the 0.95-0.99 range at the 0°C level ([Fig. 6c](#)) and reflectivity values as high as 60 dBZ ([Fig. 6a](#)), small hailstones interspersed with large rain droplets are likely occurring aloft.

Although rain is likely occurring at the ground given  $Z_{DR}$  values  $> 1.0$  dB ([Fig. 5b](#)) collocated with only 50 dBZ reflectivity echoes ([Fig. 5a](#)) and CC values ranging from 0.95-0.99 ([Fig. 5c](#)) on the lowest elevation slice, a Special Weather Statement may be issued at this time with the forecast and expectation that subsevere hail will occur at the ground as liquid water droplets are continually lofted into subfreezing temperatures and form into small hailstones as the thunderstorm updraft continues to develop and intensify.

By 2028 UTC, [Figures 8-10](#) depict the thunderstorm updraft quickly entering Stage 2 of the decision aid ([Fig. 2](#)) and beginning to grow in vertical depth. With the  $Z_{DR}$  ([Fig. 10b](#)) and  $K_{DP}$  columns ([Fig. 10d](#)) continuing to reach and slightly exceed the -10°C level, CC values in the mixed phase region of the updraft continue to depress further (0.90-0.95) signifying the continued growth of small hailstones ([Fig. 10c](#)). Reflectivity values in the updraft core have also increased with 60+ dBZ now visible just shy of the -10°C level ([Fig. 10a](#)). Additionally, the 50 dBZ echoes also appear to reach the median height threshold for severe thunderstorms as described in [Frugis](#)

[and Wasula 2011](#), although the 60 dBZ echo top falls just shy of the median height threshold.

Using the decision aid with the FSI CAPPI set at the -10°C level, the thunderstorm is capable of lofting supercooled water droplets into the hail growth zone of -10°C to -30°C ([Miller et al. 1988](#)). The  $Z_{DR}$  ([Fig. 9b](#)) and  $K_{DP}$  columns ([Fig. 9d](#)) reach the -10°C level, with 60+ dBZ reflectivity values ([Fig. 9a](#)) apparent as well as small, growing hailstones are mixed with supercooled water droplets. Further depressed CC values of 0.90-0.95 near the -10°C level ([Fig. 9c](#)) indicate that small water-coated hailstones are continuing to grow in size with  $K_{DP}$  values above 2.0 deg/km ([Fig. 10d](#)). No storm-scale rotation was apparent with this thunderstorm to enhance hail formation and growth (not shown).

On the lowest elevation slice, rain possibly mixed with small hail may be occurring at the ground as reflectivity values increase to 50-60 dBZ ([Fig. 8a](#)) collocated with  $Z_{DR}$  values of 1.0-4.0 dB ([Fig. 8b](#)), depressed CC values ranging from 0.90-0.97 ([Fig. 8c](#)), and  $K_{DP}$  values 2.0+ deg/km ([Fig. 8d](#)). Although severe hail is not likely occurring at the ground at this time, a Severe Thunderstorm Warning may be issued based on the conceptual forecast approach taken analyzing this thunderstorm.

With supercooled water droplets being continually lofted into the hail growth zone with both the  $Z_{DR}$  and  $K_{DP}$  columns reaching the -10°C level, small hailstones will continue to grow in size and reach severe limits. The favorable thermodynamic and kinematic environments further increase confidence in issuing a warning as the thunderstorm updraft will likely continue to grow and/or sustain at current levels. If the thunderstorm updraft exhibited  $Z_{DR}$  and  $K_{DP}$  columns below the -10°C level, the thunderstorm can continue to be monitored

with a Special Weather Statement already out for possible subsevere hail.

By 2047 UTC (Figs. 11-13), the thunderstorm is in Stage 3 of the decision aid (Fig. 2), maintaining an updraft capable of producing severe hail. Severe hail was reported at 2045 UTC (Fig. 11d), nearly 20 minutes after the proposed issuance of the Severe Thunderstorm Warning. The  $Z_{DR}$  (Fig. 13b) and  $K_{DP}$  columns (Fig. 13d) now reach the  $-20^{\circ}\text{C}$  level as the thunderstorm updraft is fully developed. With nearly 20 minutes of supercooled water droplets being lofted into the hail growth zone, CC values have depressed further (Fig. 13c) with a broad region of values  $CC < 0.90$  extending from the lowest elevation slice past the  $-20^{\circ}\text{C}$  level. Setting the FSI CAPPI at the  $-20^{\circ}\text{C}$  level reveals a reflectivity core of  $65+$  dBZ (Fig. 12a); also apparent on the lowest elevation slice (Fig. 11a) and within the updraft core (Fig. 13a). Despite a mature updraft, no storm-scale rotation was apparent (not shown).

The lowest elevation slice indicates that severe hail is likely occurring at the

ground, with  $65+$  dBZ (Fig. 11a) collocated with  $Z_{DR}$  values ranging from  $\sim 0.5$ - $1.5$  dB (Fig. 11b) and CC values ranging from  $\sim 0.85$ - $0.93$  (Fig. 11c).  $K_{DP}$  values as high as  $2.0$  deg/km at the  $-20^{\circ}\text{C}$  level (Fig. 12d) indicates that sufficient moisture is present for the formation and continued threat of severe hail.

A Severe Thunderstorm Warning was valid for this thunderstorm from 2041-2130 UTC. The report of severe hail at 2045 UTC resulted in a lead time of only 4 minutes. Using the conceptual forecast approach outlined in the decision aid, an improved lead time from 4 minutes to a maximum of 17 minutes could have been achieved, although the time to create and disseminate the warning could reduce the potential improved lead time. By applying a conceptual understanding of the PR numerical output, a Severe Thunderstorm Warning could have been issued early in the lifecycle of this thunderstorm by forecasting the occurrence of severe hail at the ground instead of waiting for legacy numerical thresholds to be reached.



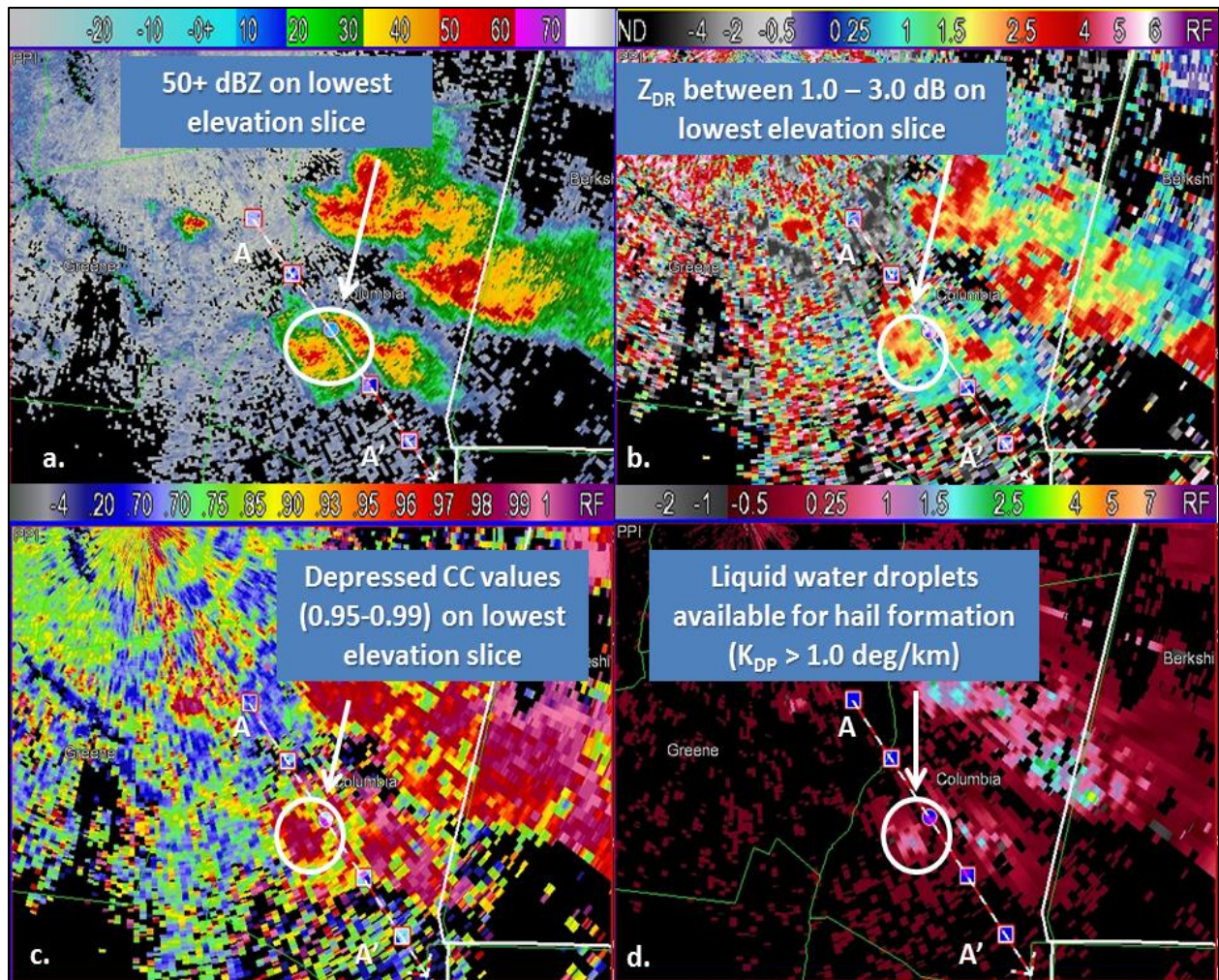


**Fig. 5.** FSI PPI  $0.5^\circ$  elevation slice from the KENX radar of the Columbia County (NY) thunderstorm valid at 2024 UTC 21 May 2013. Panels are (a) base reflectivity (dBZ), (b)  $Z_{DR}$  (dB), (c) CC (unit less), and (d)  $K_{DP}$  (deg/km). White circles denote areas of interest.

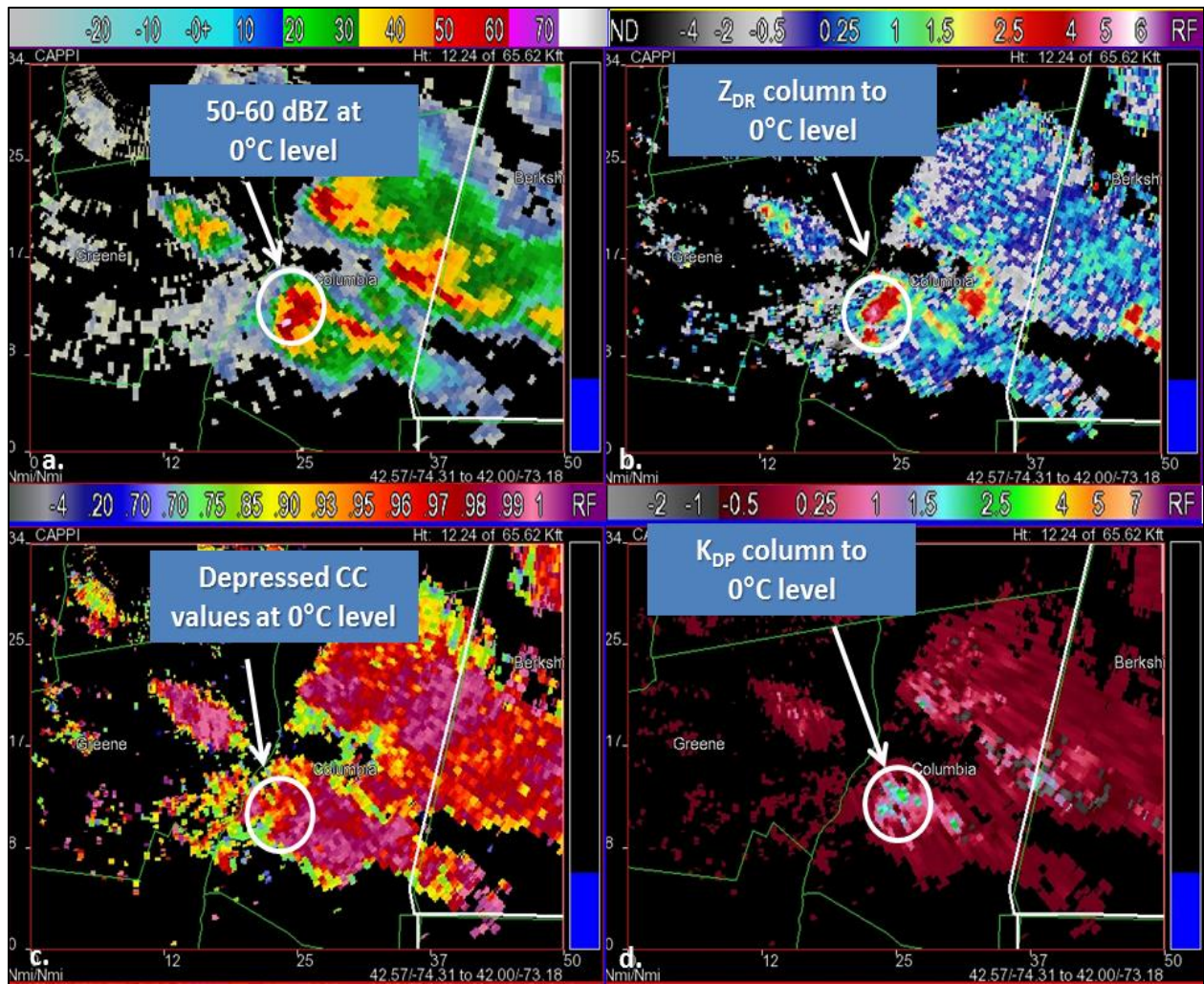


**Fig. 6.** Same as in [Fig. 5](#), except for a FSI CAPPI (constant altitude) display, set at the 0°C level.



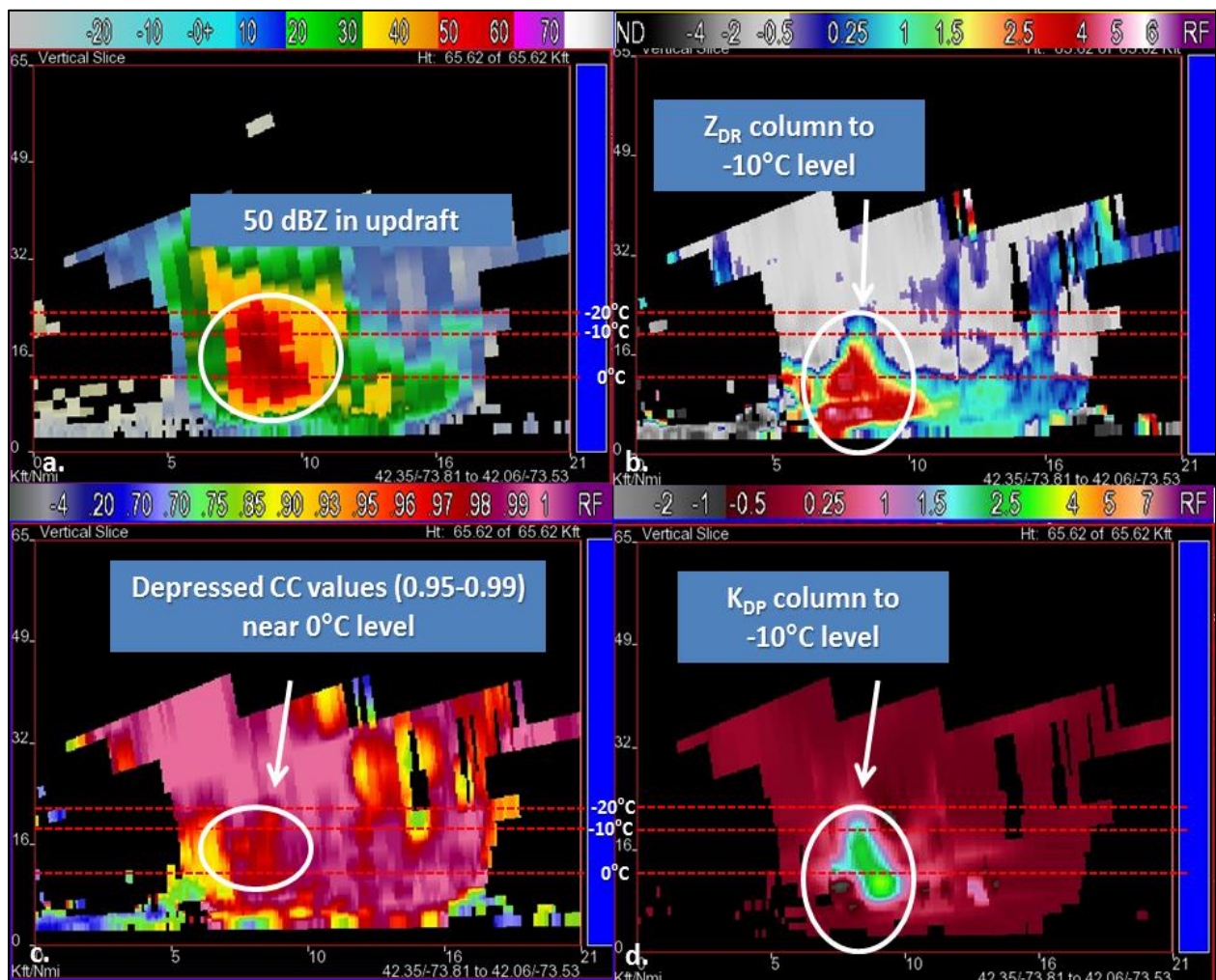


**Fig. 7.** Same as in [Fig. 5](#), except for a FSI VDX (vertical cross section) display. Dashed red lines denote temperature levels of 0°C, -10°C level, and -20°C.

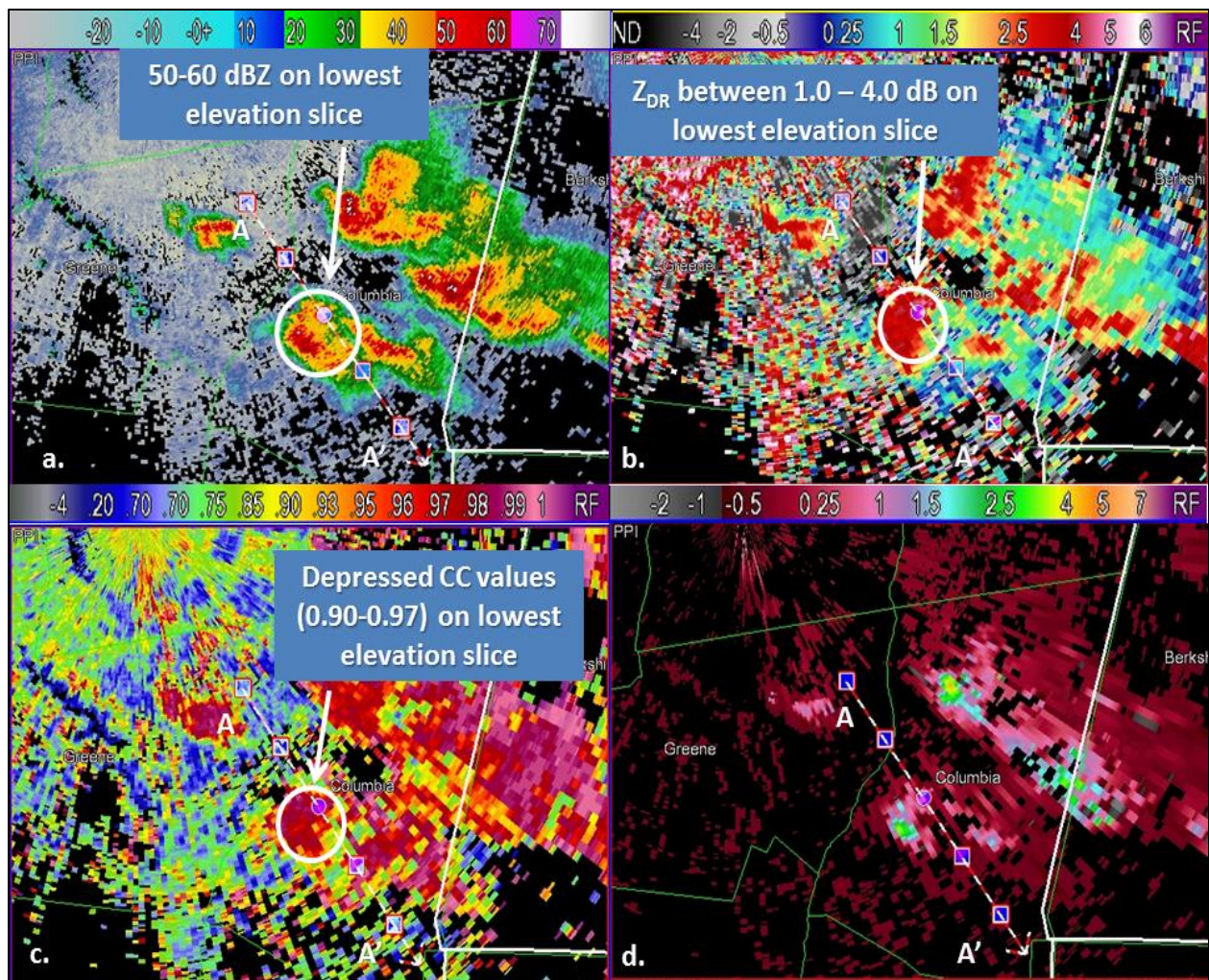


**Fig. 8.** Same as in [Fig. 5](#), except valid at 288 UTC.



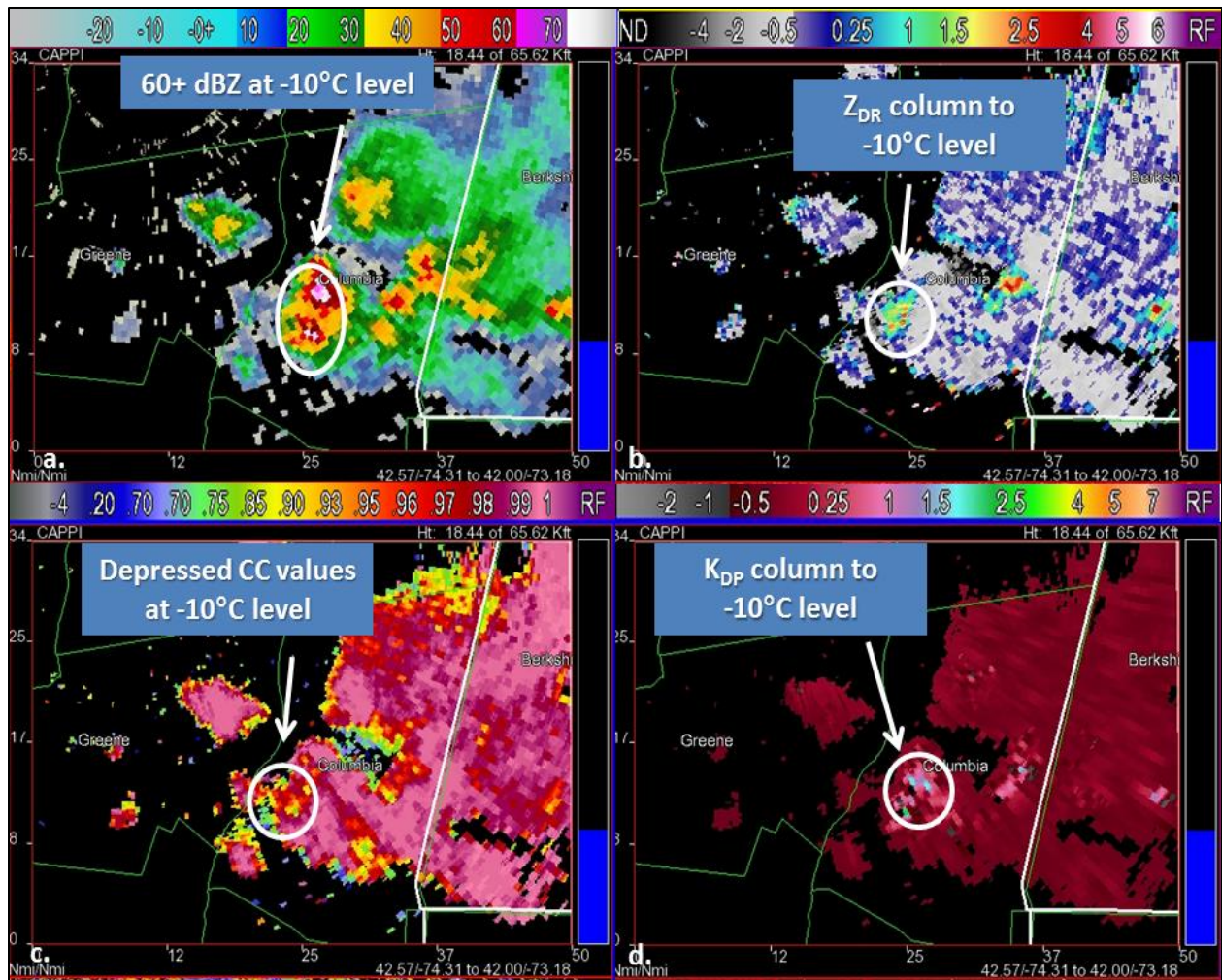


**Fig. 9.** Same as in [Fig. 5](#), except for a FSI CAPPI, set at the  $-10^{\circ}\text{C}$  level, and valid at 2028 UTC.



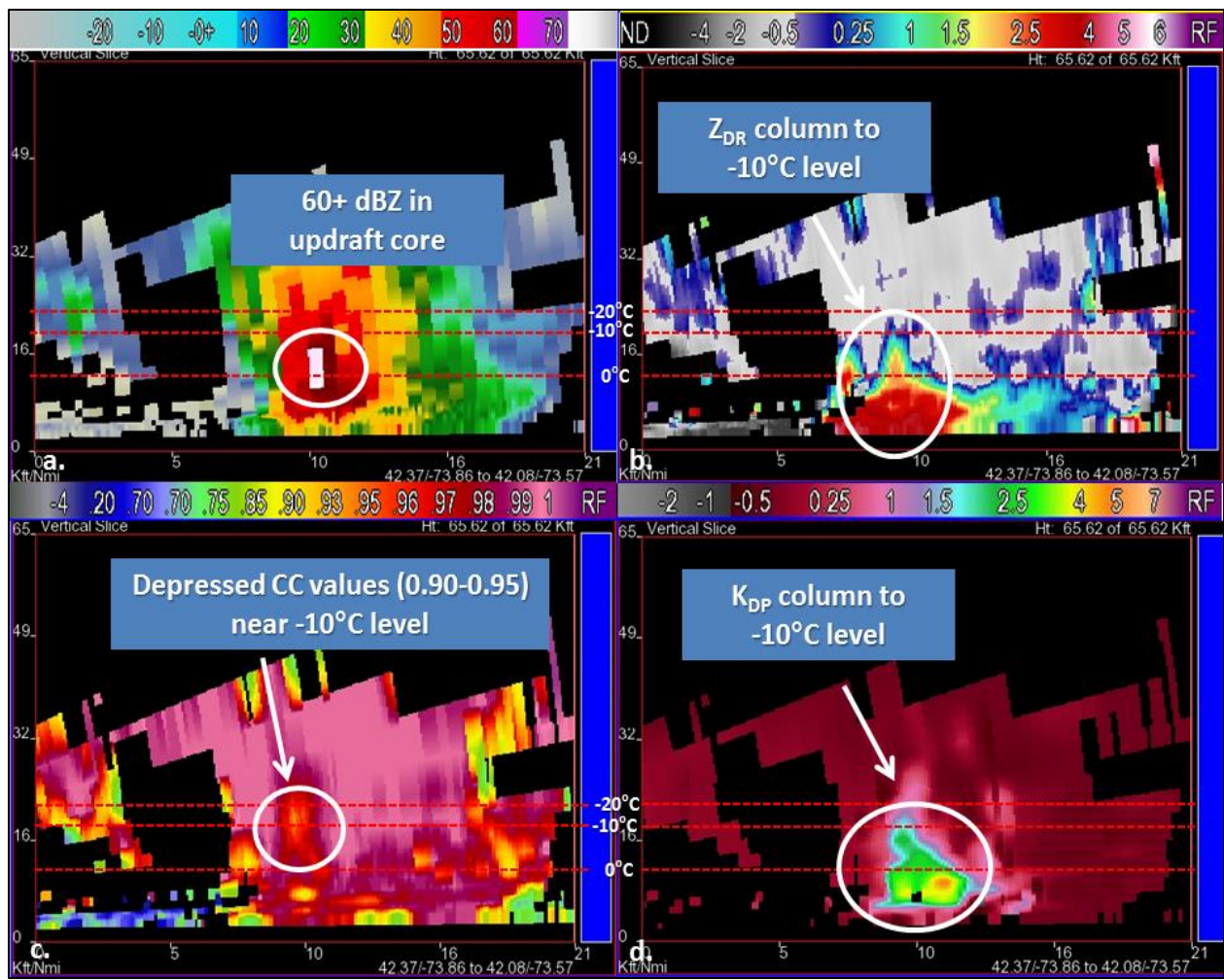


**Fig. 10.** Same as in [Fig. 5](#), except for a FSI VDX valid at 2028 UTC. Dashed red lines denote temperature levels of 0°C, -10°C level, and -20°C.

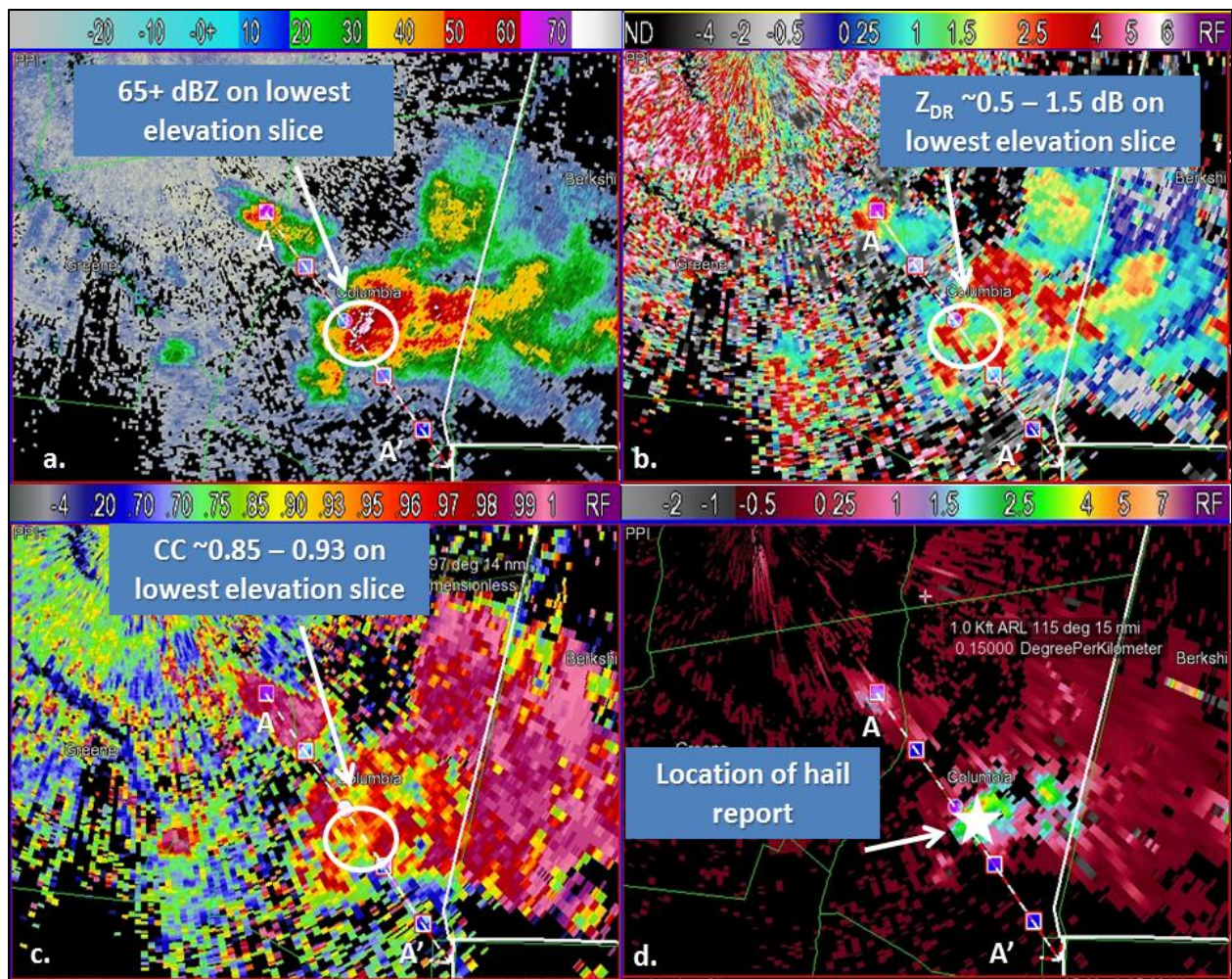
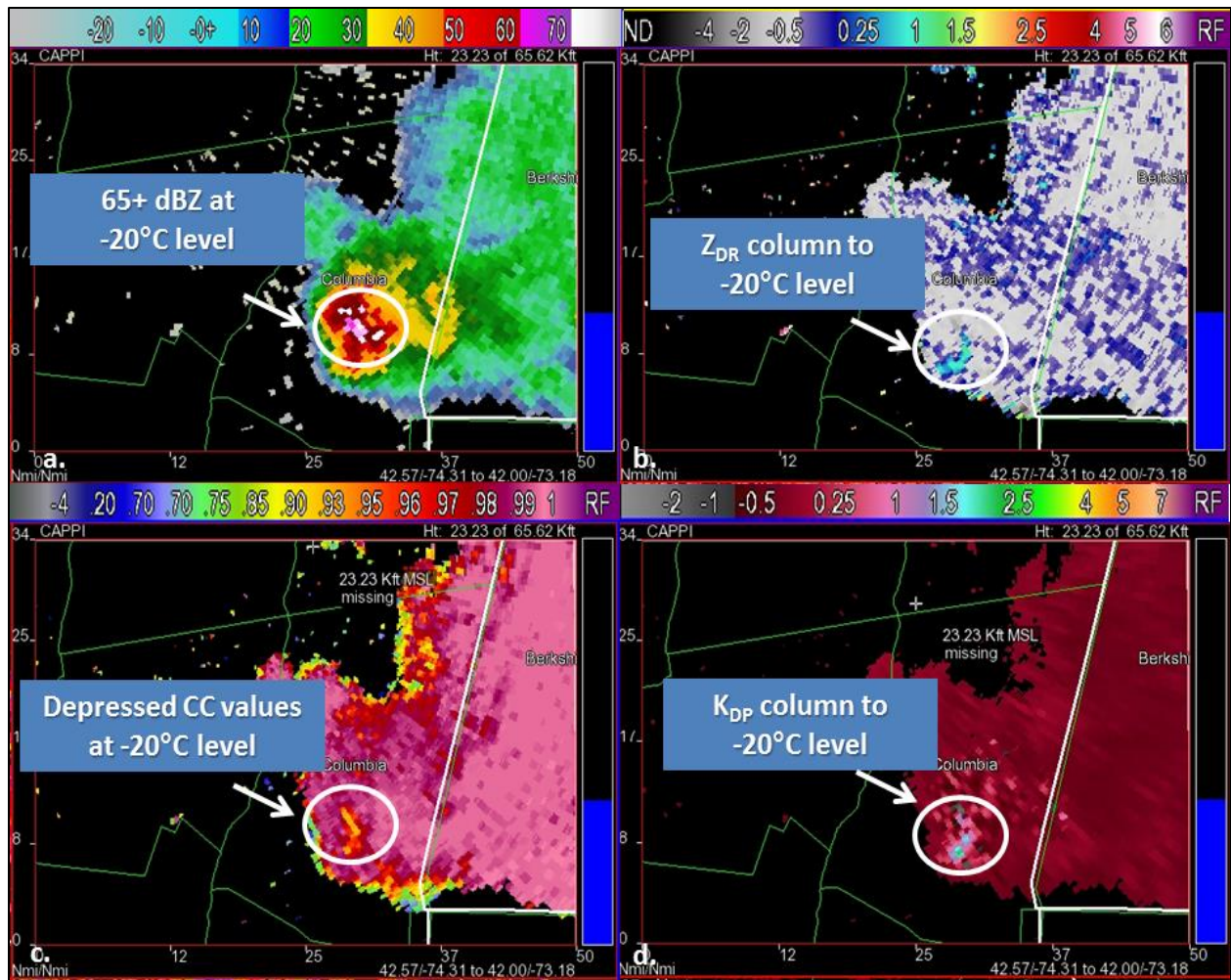
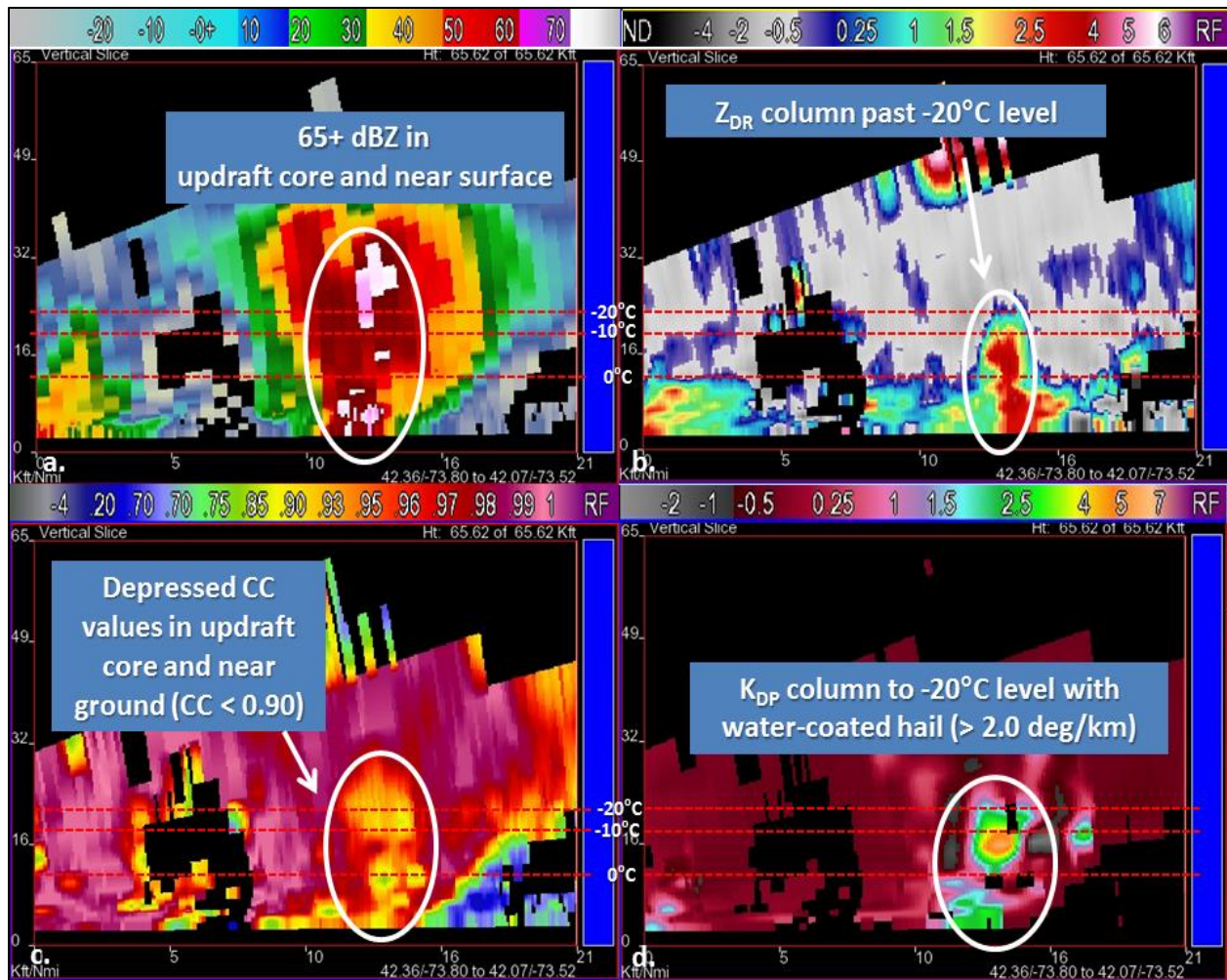


Fig. 11. Same as in Fig. 5, except valid at 2047 UTC.





**Fig. 12.** Same as in [Fig. 5](#), except for a FSI CAPPI, set at the  $-20^{\circ}\text{C}$  level, and valid at 2047 UTC.



**Fig. 13.** Same as in [Fig. 5](#), except for a FSI VDX valid at 2047 UTC. Dashed red lines denote temperature levels of 0°C, -10°C level, and -20°C.

*b) Case 2: Herkimer County, NY*

The second thunderstorm analyzed affected portions of Herkimer County in east-central NY between 2033-2110 UTC. [Figures 14-16](#) depict the thunderstorm at Stage 1 of the decision aid ([Fig. 2](#)) at 2033 UTC, with white circles denoting areas of interest. At 2033 UTC, the thunderstorm was in the updraft development and hail formation stage, with 50 dBZ echoes evident on the lowest elevation slice ([Fig. 14a](#)) and extending up to the 0°C level ([Fig. 16a](#)). Both the  $Z_{DR}$  ([Fig. 16b](#)) and  $K_{DP}$  columns ([Fig. 16d](#)) extend to the -10°C level, well

past the 0°C level. A depressed region of CC values (0.95-0.99) extends from the 0°C level to the -10°C level indicative of mixed phase hydrometeors present in the updraft core ([Fig. 16c](#)).

Using the decision aid with the FSI CAPPI set at the 0°C level, this thunderstorm is capable of lofting liquid water droplets into subfreezing temperatures for the formation of hail embryos and small hailstones, despite legacy reflectivity values remaining generally below the 0°C level. The  $Z_{DR}$  ([Fig. 15b](#)) and  $K_{DP}$  columns ([Fig. 15d](#)) reach the 0°C level, with liquid water droplets readily available for the formation

of hail embryos and small hailstones. With depressed CC values in the 0.92-0.99 range at the 0°C level (Fig. 15c) and reflectivity values as high as 50 dBZ (Fig. 15a), small hailstones interspersed with large rain droplets are likely occurring aloft.

Although rain is likely occurring at the ground given  $Z_{DR}$  values  $> 1.0$  dB (Fig. 14b) collocated with only 50 dBZ reflectivity echoes (Fig. 14a) and CC values ranging from 0.95-0.99 (Fig. 14c) on the lowest elevation slice, a Special Weather Statement may be issued at this time with the forecast and expectation that subsevere hail will occur at the ground as liquid water droplets are continually lofted into subfreezing temperatures and form into small hailstones as the thunderstorm updraft continues to develop and intensify.

By 2042 UTC, Figures 17-19 depict the thunderstorm updraft entering Stage 2 of the decision aid (Fig. 2) and beginning to grow in vertical depth, despite intensifying at a slower rate compared to Storm 1 given the same thermodynamic and kinematic environments. With the  $Z_{DR}$  (Fig. 19b) and  $K_{DP}$  columns (Fig. 19d) increasing in vertical depth to reach the -20°C level, CC values in the mixed phase region of the updraft continue to depress further (0.90-0.95) signifying the continued growth of small hailstones (Fig. 19c). Reflectivity values in the updraft core have also increased with 60+ dBZ now visible between the -10°C and -10°C levels (Fig. 19a). Additionally, the 50 and 60 dBZ echoes also reach the median height threshold for severe thunderstorms as described in Frugis and Wasula 2011 at 2042 UTC.

Using the decision aid with the FSI CAPPI set at the -10°C level, the thunderstorm is capable of lofting supercooled water droplets into the hail growth zone of -10°C to -30°C (Miller et al. 1988). The  $Z_{DR}$  (Fig. 18b) and  $K_{DP}$  columns

(Fig. 18d) reach the -10°C level, with 60+ dBZ reflectivity values (Fig. 18a) apparent as well as small, growing hailstones are mixed with supercooled water droplets. Depressed CC values continue near the -10°C level (Fig. 18c) indicating that small water-coated hailstones are continuing to grow in size with  $K_{DP}$  values above 1.0 deg/km (Fig. 18d). Storm-scale rotation via a developing mesocyclone was also now apparent with this thunderstorm to enhance the hail formation and growth process (not shown).

On the lowest elevation slice, rain possibly mixed with small hail may be occurring at the ground as reflectivity values increase to 50-60 dBZ (Fig. 17a) collocated with  $Z_{DR}$  values of 0.5-3.0 dB (Fig. 17b), depressed CC values ranging from 0.90-0.95 (Fig. 17c), and  $K_{DP}$  values around 1.0 deg/km (Fig. 17d). Although severe hail is not likely occurring at the ground at this time, a Severe Thunderstorm Warning may be issued based on the conceptual forecast approach taken analyzing this thunderstorm. With supercooled water droplets being continually lofted into the hail growth zone with both the  $Z_{DR}$  and  $K_{DP}$  columns easily reaching the -10°C level and approaching the -20°C level, small hailstones will continue to grow in size and reach severe limits. A developing mesocyclone along with favorable thermodynamic and kinematic environments further increase confidence in issuing a warning at this time as the thunderstorm updraft will likely continue to grow and/or sustain at current levels, with nonhydrostatic pressure differences contributing to the hail formation process.

By 2110 UTC (Figs. 20-22), the thunderstorm is in Stage 3 of the decision aid (Fig. 2), maintaining a mature updraft capable of producing severe hail. Severe hail was reported at 2115 UTC (Fig. 20d), nearly 35 minutes after the proposed



issuance of the Severe Thunderstorm Warning. With a continued mesocyclone present with the thunderstorm (not shown), hail has grown to severe limits within the updraft core with a large region of 65+ dBZ extending from the lowest elevation slice past the  $-20^{\circ}\text{C}$  level (Fig. 22a). A TBSS is also now apparent with the FSI CAPPI set at the  $-20^{\circ}\text{C}$  level, with CC values dropping below 0.80 (Fig. 21c) along with a spike in  $Z_{\text{DR}}$  (Fig. 21b) and reflectivity values (Fig. 21a) down radial of the thunderstorm updraft. A further indication that severe hail exists in the thunderstorm updraft is  $Z_{\text{DR}}$  values near 0 dB revealing tumbling hailstones aloft (Fig. 22b).

The lowest elevation slice indicates that severe hail is likely occurring at the ground, with 65+ dBZ (Fig. 20a) collocated with  $Z_{\text{DR}}$  values ranging from  $\sim 0.0$ -1.0 dB (Fig. 20b) and CC values ranging from  $\sim 0.80$ -0.90 (Fig. 20c). With  $K_{\text{DP}}$  values as high as 2.0-3.0 deg/km on the lowest

elevation slice (Fig. 20d), severe hailstones are possibly melting below the beam, but likely remaining at severe levels given low CC values ( $< 0.90$ ) on the lowest elevation slice and the presence of a TBSS aloft.

A Severe Thunderstorm Warning was valid for this thunderstorm from 2106-2200 UTC. The report of severe hail at 2115 UTC resulted in a lead time of 9 minutes. Using the conceptual forecast approach outlined in the decision aid, an improved lead time from 9 minutes to a maximum of 33 minutes could have been achieved by applying a conceptual understanding and forecast methodology of the PR numerical output. Even though legacy thresholds were reached, utilizing the PR methodology can further increase confidence in issuing a Severe Thunderstorm Warning. As discussed with Case 1, the time to create and disseminate the warning could reduce the potential improved lead time.

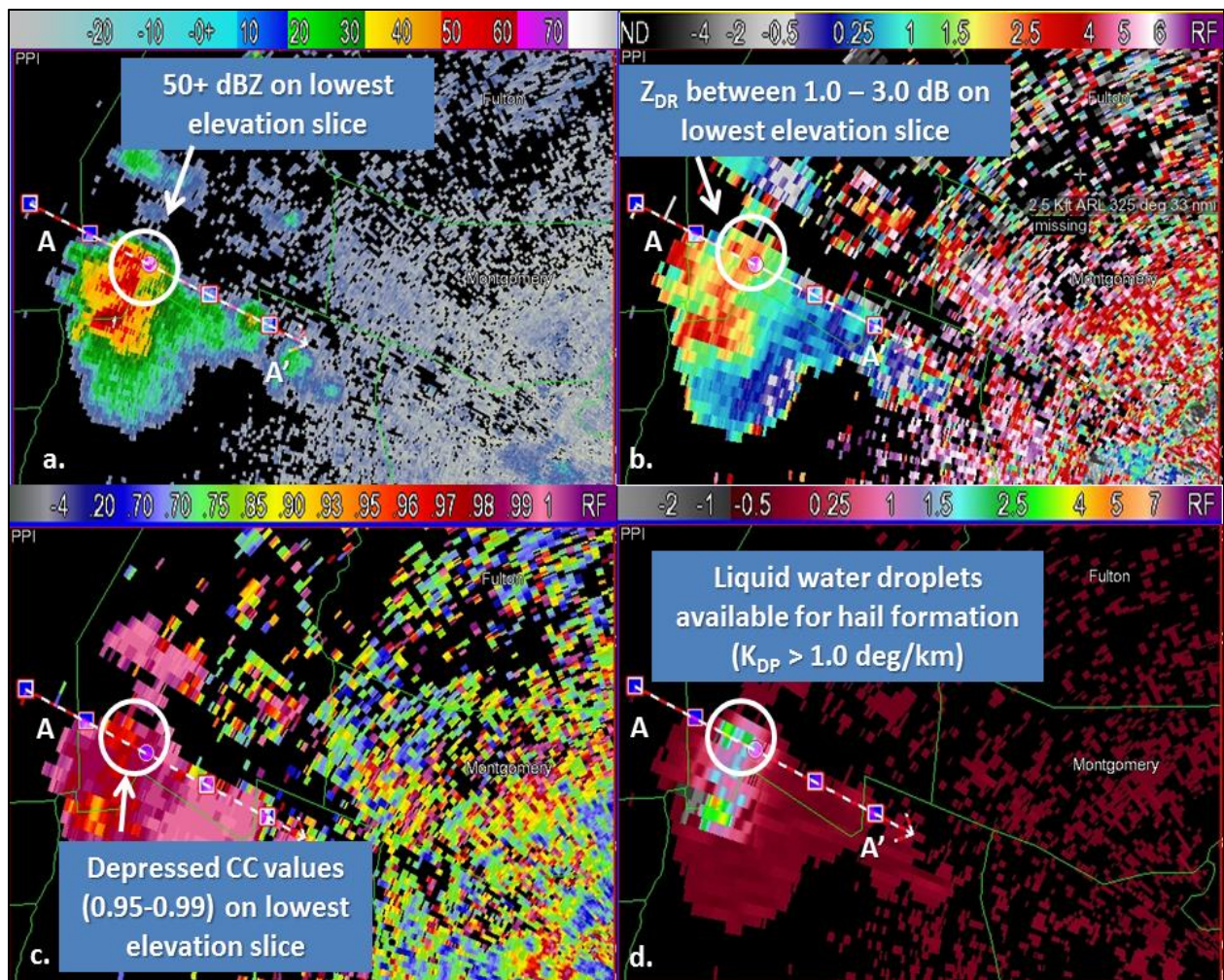


**Fig. 14.** FSI PPI 0.5° elevation slice from the KENX radar of the Herkimer County (NY) thunderstorm valid at 2033 UTC 21 May 2013. Panels are (a) base reflectivity (dBZ), (b)  $Z_{DR}$  (dB), (c) CC (unit less), and (d)  $K_{DP}$  (deg/km). White circles denote areas of interest.

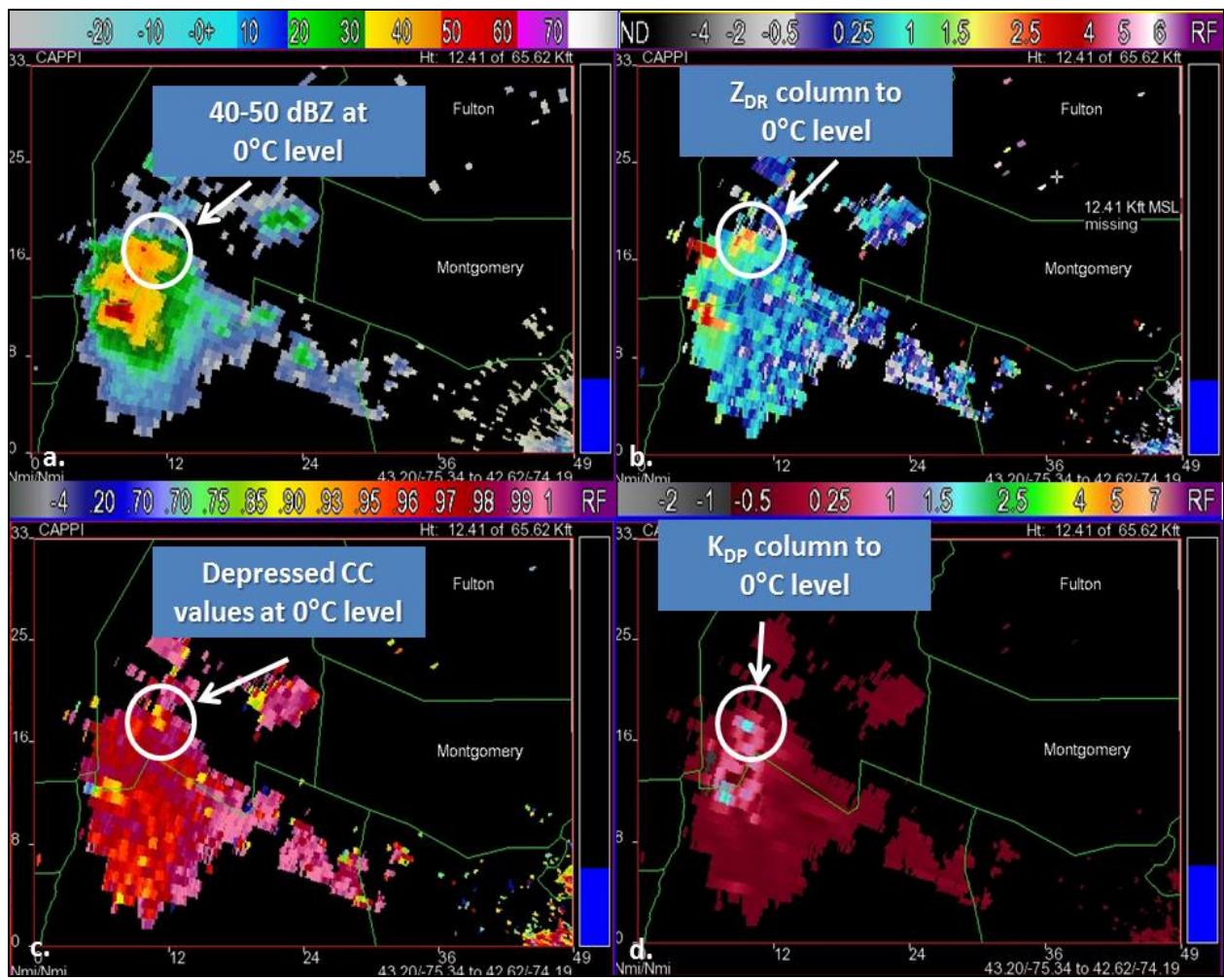


**Fig. 15.** Same as [Fig. 14](#) except for a FSI CAPPI (constant altitude) display, set at the 0°C level.



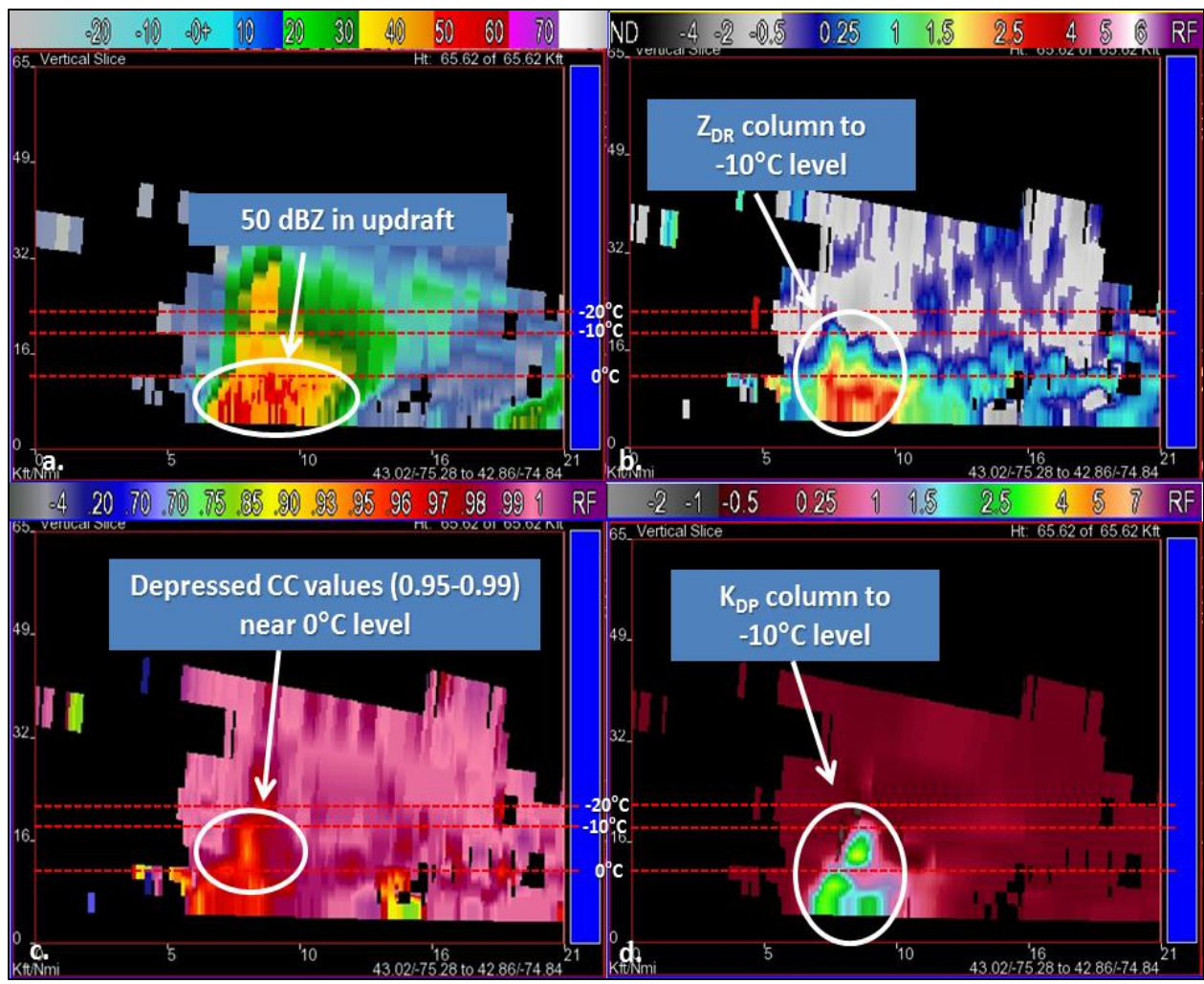


**Fig. 16.** Same as Fig. 14, except for a FSI VDX (vertical cross section) display. Dashed red lines denote temperature levels of 0°C, -10°C level, and -20°C.

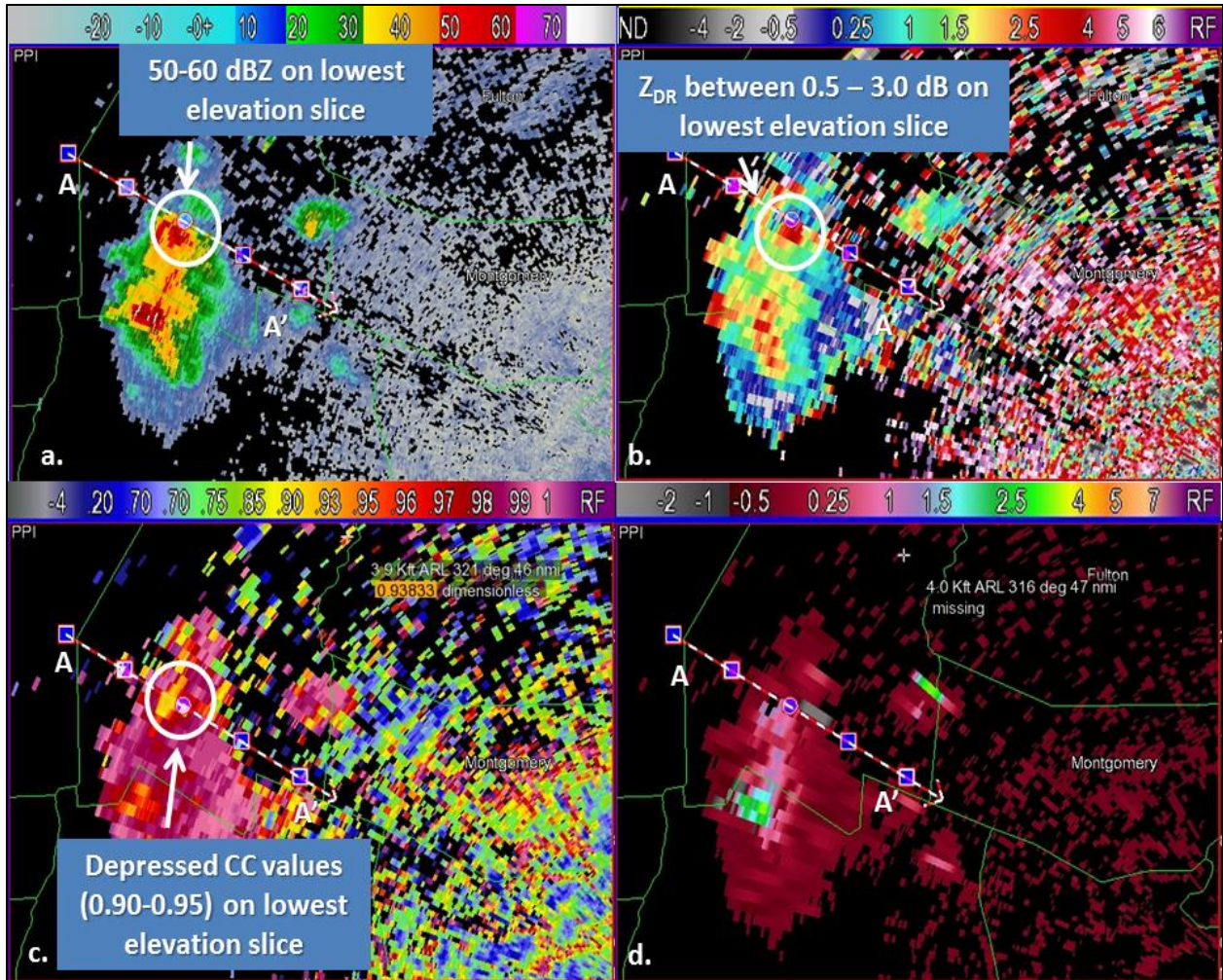
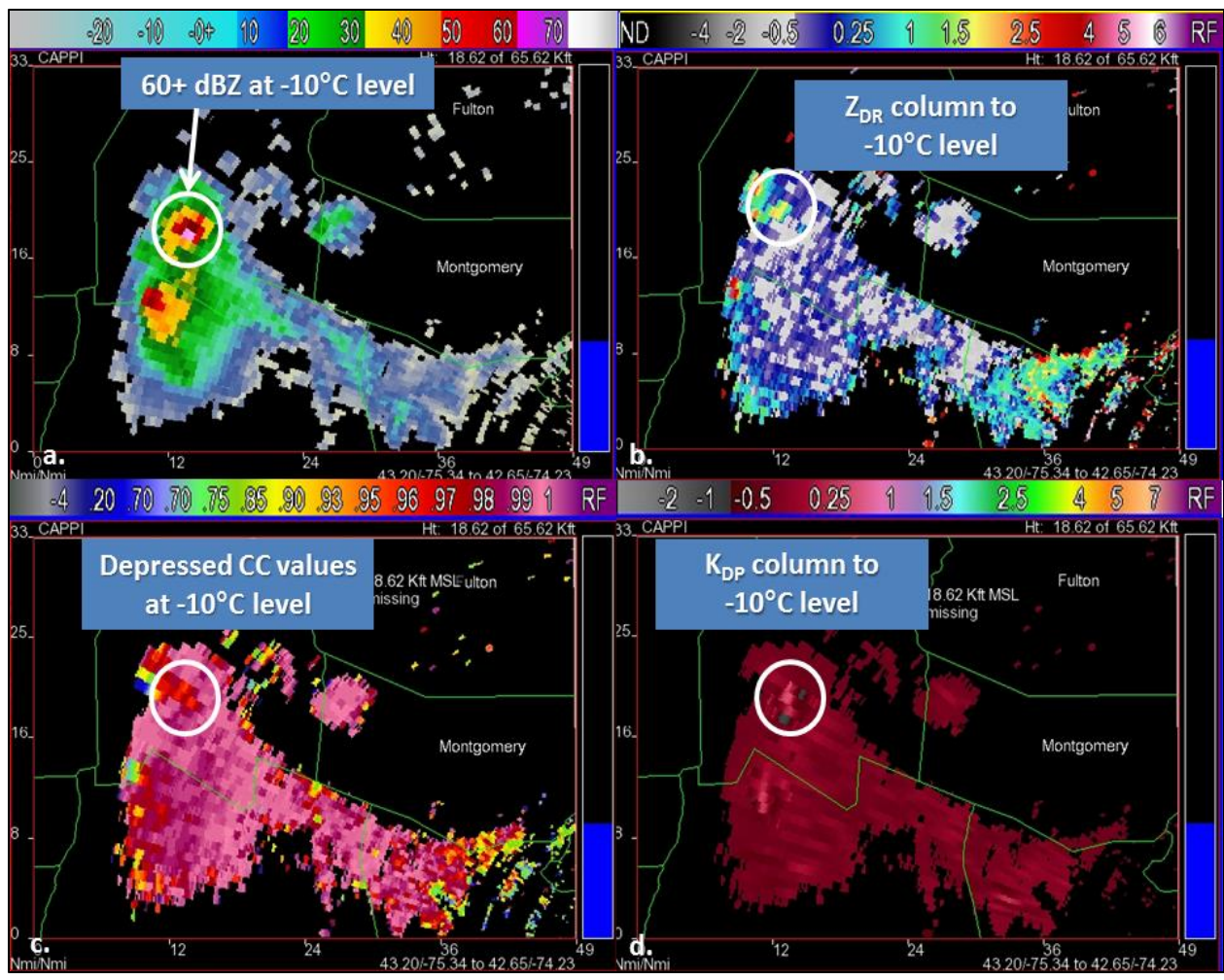


Fig. 17. Same as Fig. 14, except valid at 2042 UTC.





**Fig. 18.** Same as [Fig. 14](#) except for a FSI CAPPI, set at the -10°C level, and valid at 2042 UTC.



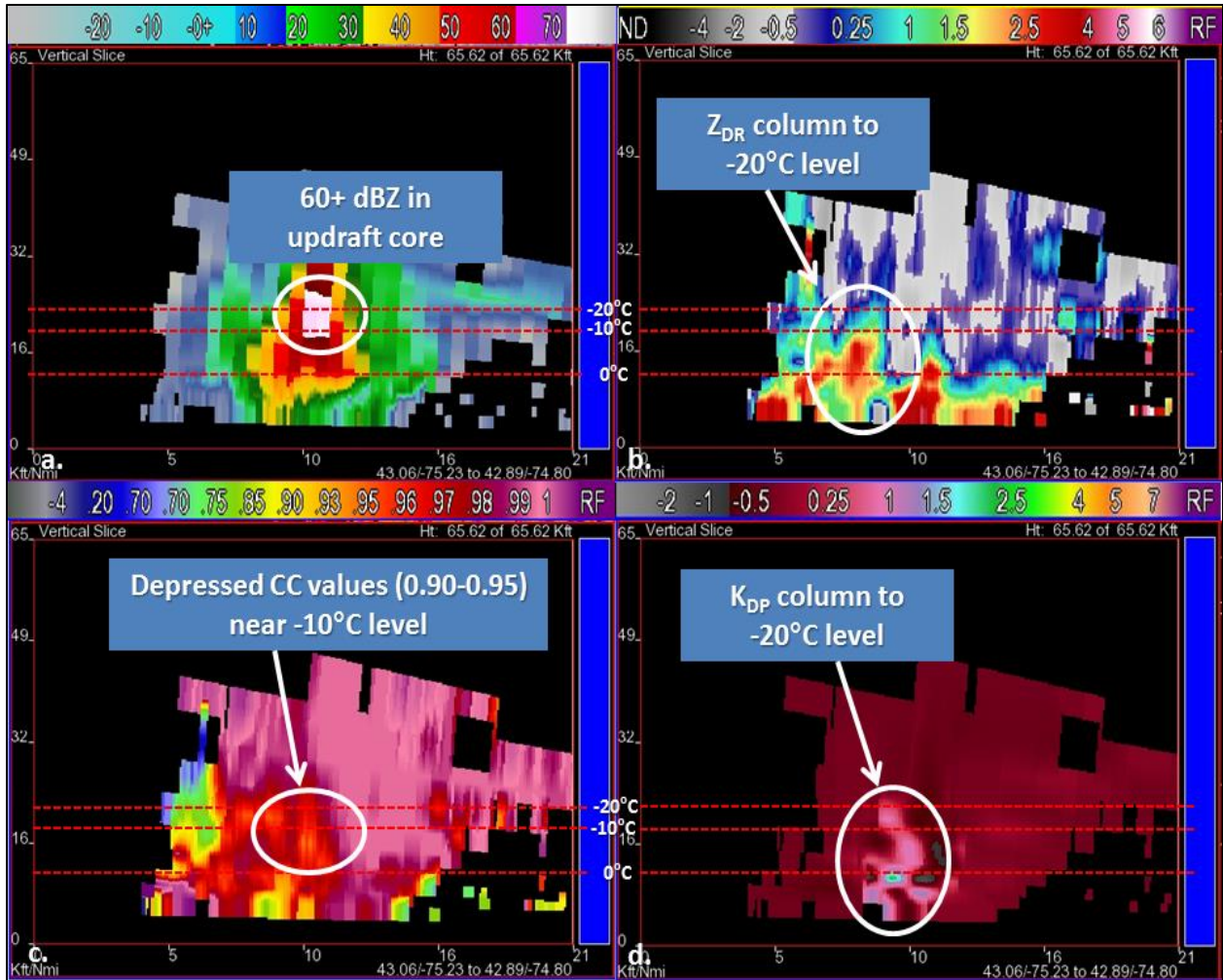


**Fig. 19.** Same as in Fig. 14, except for a FSI VDX valid at 2042 UTC. Dashed red lines denote temperature levels of 0°C, -10°C level, and -20°C.

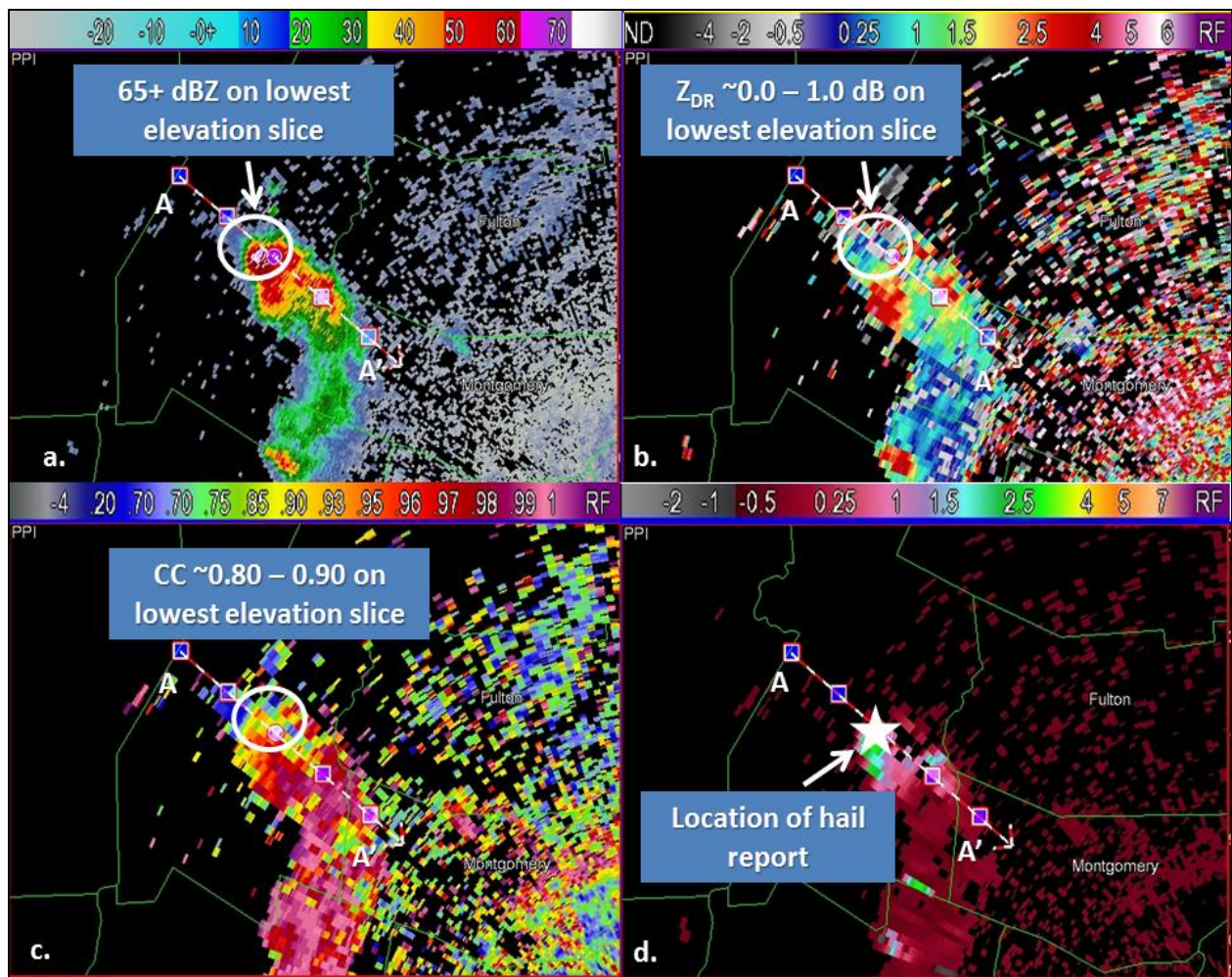


**Fig. 20.** Same as in [Fig. 14](#), except valid at 2110 UTC.

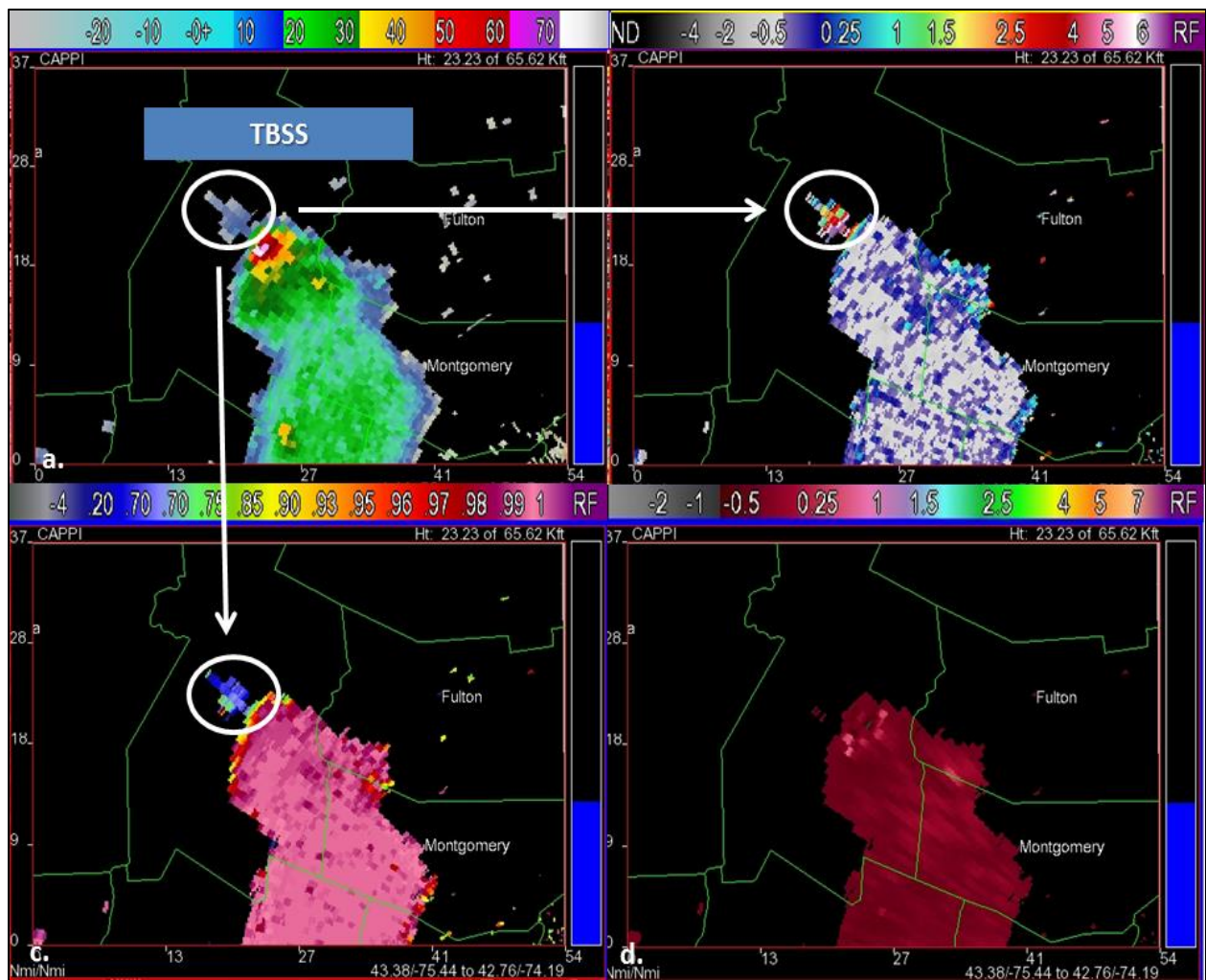


**Fig. 21.** Same as in [Fig. 14](#), except for a FSI CAPPI, set at the  $-20^{\circ}\text{C}$  level, and valid at 2110 UTC.



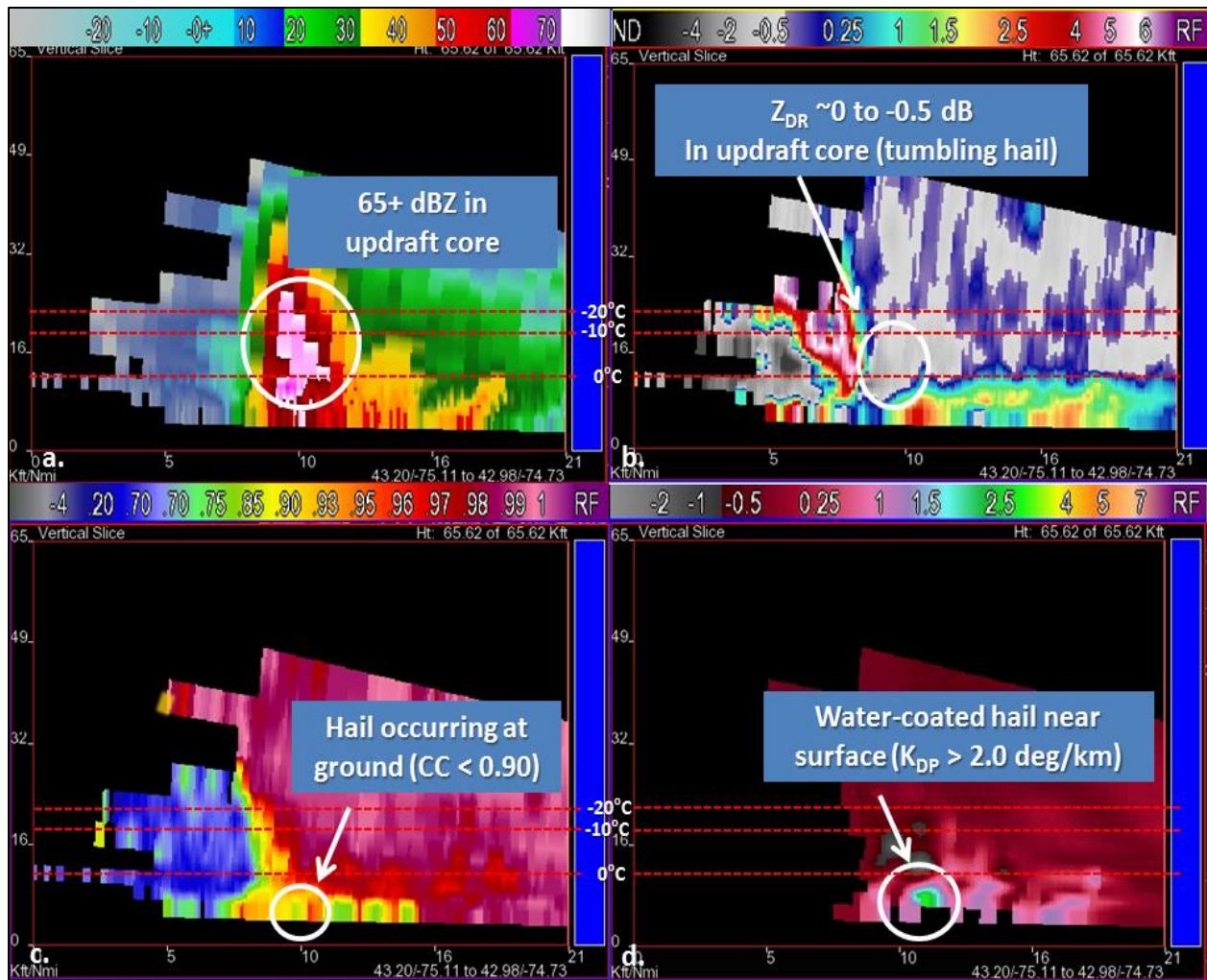


**Fig. 22.** Same as in Fig. 14 except for a FSI VDX valid at 2110 UTC. Dashed red lines denote temperature levels of 0°C, -10°C level, and -20°C.

## 5. Discussion

The proposed conceptual forecast approach and decision aid introduced for the issuance of Severe Thunderstorm Warnings for severe hail highlights the significance that PR data can have in the warning process. By tracking various PR features and correlating them to conceptual models while maintaining a situational awareness of the near-storm environment, this strategy may provide a method for forecasting severe hail occurrence at the ground early in the lifecycle of a thunderstorm.

Radar limitations such as attenuation, distance from the radar, non-uniform beam filling, and depolarization among many others must be taken into consideration when applying this proposed strategy as they can limit its usefulness. Environmental factors such as low freezing levels may also present issues with the proposed strategy and it is recommended to apply this strategy only during the warm season. The complications associated with heterogeneous ice nucleation must also be taken into consideration as certain thermodynamic environments may favor the hail growth zone beginning at temperatures

warmer than  $-10^{\circ}\text{C}$ . Additional unaccounted thunderstorm dynamics and environmental factors (i.e. cool season thunderstorms, low-topped supercells, dry hail, etc.) may also introduce error into the proposed strategy with severe hail occurring at reflectivities  $< 60$  dBZ. Expected occurrence of hail at the surface is also dependent on factors such as hailstone size and fall speed in relation to updraft strength and the near-storm environment ([MH80; Miller et al. 1988](#)).

The decision aid is meant to assist in the warning interrogation process and is not recommended to be used as the only radar warning technique. Legacy techniques, such as [Frugis and Wasula 2011](#), should still be used with the proposed new strategy allowing for the use of additional data and adding more confidence as was the case in the Herkimer County, NY thunderstorm. The availability and timing of severe hail reports also plays a large role in lead times and subsequently verifying warnings. While using the decision aid, warning

## Acknowledgements

The author would like to thank Warren Snyder, NWS Albany, NY SOO and NWS Eastern Region SSD for their reviews of this publication. The author also thanks the three anonymous reviewers from Eastern NWS Region for their helpful suggestions and comments to improve this publication. In addition, the author would like to thank NWS Albany, NY forecasters Tom Wasula, Neil Stuart, and Brian Frugis for their insight and review of this paper.

meteorologists must keep a vigilant situational awareness to limit potential missed events. It is also important to use all available radar and observation data, such as derived variables and lightning data.

While it is possible for additional lead time using the proposed strategy, further validation and analysis of additional cases is needed. Additionally, time requirements to create and disseminate Severe Thunderstorm Warnings and/or Special Weather Statements may also limit possible improved lead times and could also be affected by other factors such as varying thunderstorm evolutions, intensities, and timeliness of storm reports. Further examination of this method may be explored in the future, with the decision aid applied to a larger dataset of cases. The strategy described in this paper may be applicable to other county warning areas with different local thermodynamic and geographic effects as well, with further research that could be performed to test its validity.

## References

- Boustead, J. M., 2008: Using maximum storm-top divergence and the vertical freezing level to forecast hail size. Preprints, *24th Conf. on Severe Local Storms*, Savannah, GA, Amer. Meteor. Soc., P6.6.
- Cerniglia, C.S. and W.R. Snyder, 2002: Development of warning criteria for severe pulse thunderstorms in the northeastern United States using the WSR-88D. *Eastern Region Technical Attachment, No. 2002-03*, National Weather Service, NOAA, Department of Commerce, 14 pp., Bohemia, NY. [Available online at

- <http://www.erh.noaa.gov/er/hq/ssd/erps/ta/ta2002-03.pdf>].
- Changnon, S. A., 1970: Hailstreaks. *J. Atmos. Sci.*, **27**, 109-125.
- Donavon, R. A., and K. A. Jungbluth, 2007: Evaluation of a technique for radar identification of large hail across the upper Midwest and central Plains of the United States. *Wea. Forecasting*, **22**, 244-254.
- Frugis, B. J., and T. A. Wasula, 2011: Development of warning thresholds for one inch or greater hail in the Albany, New York county warning area. *Eastern Region Technical Attachment, No. 2011-05*, National Weather Service, NOAA, Department of Commerce, 20 pp., Bohemia, NY. [Available online at <http://www.erh.noaa.gov/er/hq/ssd/erps/ta/ta2011-05.pdf>].
- Hart, J. A., and W. Korotky, 1991: The SHARP workstation v1.50 users guide. National Weather Service, NOAA, 30pp.
- Hayes, J. C., 2008: Hail in the Gray, Maine county warning area. *Eastern Region Technical Attachment, No. 2008-04*, National Weather Service, NOAA, Department of Commerce, 22 pp., Bohemia, NY. [Available online at <http://www.erh.noaa.gov/er/hq/ssd/erps/ta/ta2008-04.pdf>].
- Holton, J. R., 1992. *An Introduction to Dynamic Meteorology*. Academic Press Inc.
- Hubbert, J., V. N. Bringi, L. D. Carey, and S. Bolen, 1998: CSU-CHILL polarimetric radar measurements from a severe hail storm in eastern Colorado. *J. Appl. Meteor.*, **37**, 749-775.
- Johns, R. H., and C. A. Doswell III, 1992: Severe local storms forecasting. *Wea. Forecasting*, **7**, 588-612.
- Kramar, M. R., and J. J. Waters, 2009: Predicting severe hail in the WFO LWX county warning area: toward increased accuracy in hail size forecasts. Preprints, *24<sup>th</sup> Conf. on Hydrology*, Atlanta, GA, Amer. Meteor. Soc., 447.
- Lahiff, C. T., 2005: Vertically integrated liquid density and its associated hail size range across the Burlington, Vermont county warning area. *Eastern Region Technical Attachment, No. 2005-01*, National Weather Service, NOAA, Department of Commerce, 20 pp., Bohemia, NY. [Available online at <http://www.erh.noaa.gov/er/hq/ssd/erps/ta/ta2005-01.pdf>].
- Kumjian, M. R., and A. V. Ryzhkov, 2008: Polarimetric signatures in supercell thunderstorms. *J. Appl. Meteor.*, **47**, 1940-1961.
- Kumjian, M. R., 2013a: Principles and applications of dual-polarization weather radar. Part I: Description of the polarimetric radar variables. *J. Operational Meteor.*, **1** (19), 226-242.
- \_\_\_\_\_, 2013b: Principles and applications of dual-polarization weather radar. Part II: Warm- and cold-season applications. *J. Operational Meteor.*, **1** (20), 243-264.
- Lemon, L. R., 1977: New severe thunderstorm radar identification techniques and warning criteria. *NOAA Tech Memo. NWS NSSFC-1*. Kansas City, MO. NOAA National Severe Storms Forecast Center.



- \_\_\_\_\_, 1998: The radar “three-body scatter spike”: An operational large hail signature. *Wea. Forecasting*, **13**, 327-340.
- Markowski, P. and Y. Richardson, 2010: *Mesoscale Meteorology in Midlatitudes*. Wiley-Blackwell, 424 pp.
- Matson, R. J. and A. W. Huggins, 1980: The direct measurement of the sizes, shapes and kinematics of falling hailstones. *J. Atmos. Sci.*, **37**, 1107–1125.
- Miller, L. Jay, J. D. Tuttle, and C. A. Knight, 1988: Airflow and hail growth in a severe northern High Plains supercell. *J. Atmos. Sci.*, **45**, 736–762.
- Picca, J., and A. Ryzhkov, 2012: A dual-wavelength polarimetric analysis of the 16 May 2010 Oklahoma City extreme hailstorm. *Mon. Wea. Rev.*, **140**, 1385–1403.
- Porter, D. L., M. R. Kramar, and S. D. Landolt, 2005: Predicting severe hail for the southern High Plains and West Texas. Preprints, *32nd Conf. on Radar Meteorology*, Albuquerque, NM, Amer. Meteor. Soc. P3R.8.
- Rinehart, R. E., 2010: *Radar for Meteorologists*. 5<sup>th</sup> Edition. Rinehart Publications, 482 pp.
- Scharfenberg, K. A., and Coauthors, 2005: The Joint Polarization Experiment: Polarimetric radar in forecasting and warning decision making. *Wea. Forecasting*, **20**, 775–788.
- Straka, J. M., D. S. Zrnić, and A. V. Ryzhkov, 2000: Bulk hydrometeor classification and quantification using polarimetric radar data: synthesis of relations. *J. Appl. Meteor.*, **39**, 1341–1372.
- Stumpf, G. J., M. T. Filiaggi, V. Lakshmanan, W. F. Roberts, M. J. Istok, and S. B. Smith, 2004: A four-dimensional radar analysis tool for AWIPS. Preprints, *22nd Conf. on Severe Local Storms*, Hyannis, MA, Amer. Meteor. Soc., 8B.6.
- Stumpf, G. J., M. T. Filiaggi, M. A. Magsig, K. D. Hondl, S. B. Smith, R. Toomey, and C. Kerr, 2006: Status on the integration of the NSSL four dimensional stormcell investigator (FSI) into AWIPS. Preprints, *23rd Conf. on Severe Local Storms*, St. Louis, MO, Amer. Meteor. Soc., 8.3.
- Thompson, R. L., R. Edwards, J. A. Hart, K. L. Elmore, and P. Markowski, 2003: Close proximity soundings within supercell environments obtained from the Rapid Update Cycle. *Wea. Forecasting*, **18**, 1243–1261.
- U.S. Department of Commerce, National Weather Service Directive 10-511, *WFO Severe Weather Products Specification*. [Available online at <http://www.nws.noaa.gov/directives/sym/pd01005011curr.pdf>].
- U.S. Department of Commerce, National Weather Service Directive 10-517, *Multi-Purpose Weather Products Specification*. [Available online at <http://www.nws.noaa.gov/directives/sym/pd01005017curr.pdf>].
- U.S. Department of Commerce, Precipitable Water Plots (2013). Retrieved 19 July 2013, from National Weather Service: <http://www.crh.noaa.gov/unr/?n=pw>

- U.S. Department of Commerce, Radar Operations Center, WSR-88D Dual Polarization Deployment Progress (2013). Retrieved 18 July 2013, from National Weather Service: <http://www.roc.noaa.gov/wsr88d/PublicDocs/DualPol/DPstatus.pdf>
- U.S. Department of Commerce, Storm Prediction Center, Severe Weather Events Archive (2013). Retrieved 23 April 2014, from Storm Prediction Center: <http://www.spc.noaa.gov/exper/archive/event.php?date=20130521>
- U.S. Department of Commerce, Warning Decision Training Branch (2013). Retrieved 27 February 2015, from Warning Decision Training Branch: <http://www.wdtb.noaa.gov/courses/dualpol/Products/KDP/player.html>
- U.S. Department of Commerce, Weather Prediction Center, Surface Analysis Archive (2013). Retrieved 23 April 2014, from Weather Prediction Center: [http://www.hpc.ncep.noaa.gov/archives/web\\_pages/sfc/sfc\\_archive\\_maps.php?arcdte=05/21/2013&selmap=2013052118&maptype=namussfc](http://www.hpc.ncep.noaa.gov/archives/web_pages/sfc/sfc_archive_maps.php?arcdte=05/21/2013&selmap=2013052118&maptype=namussfc)
- Witt, A., and S. P. Nelson, 1991: The Use of Single-Doppler Radar for Estimating Maximum Hailstone Size. *J. Appl. Meteor.*, **30**, 425–431.
- Witt, A., 1996: The relationship between low-elevation WSR-88D reflectivity and hail at the ground using precipitation observations from the VORTEX project. Preprints, *18th Conf. on Severe Local Storms*, San Francisco, CA, Amer. Meteor. Soc., 183-185.